AD-A121 388 THE ACCURACY OF SEASAT 1 ALTIMETER ALTITUDE 1/1
MEASUREMENTS UNDER VARIOUS SE..(U) ROYAL AIRCRAFT
ESTABLISHMENT FARNBOROUGH (ENGLAND) G C WHITE MAY 82
UNCLASSIFIED RAE-TR-82059 DRIC-BR-84668 F/G 8/3 NL

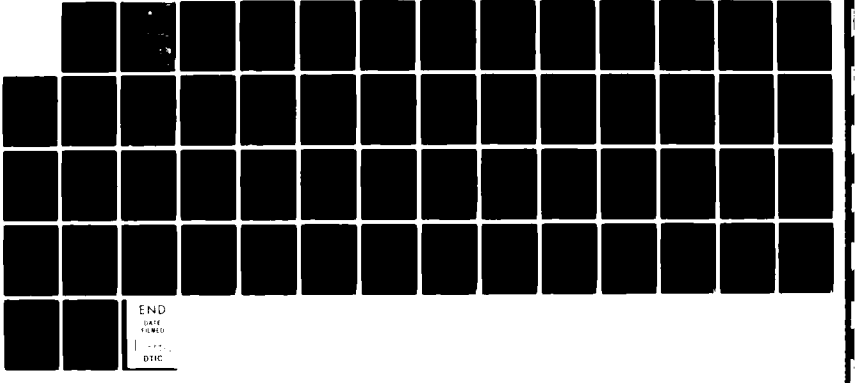

END
DATE FILMED
DTIC

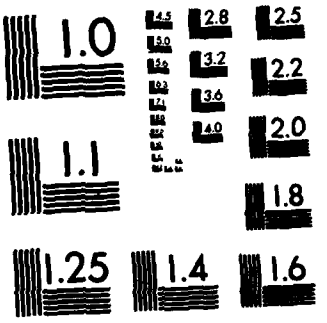

ROYAL AIRCRAFT ESTABLISHMENT

Technical Report 82060

May 1982

THE ACCURACY OF SEASAT-1 ALTIMETER ALTITUDE MEASUREMENTS UNDER VARIOUS SEA STATE CONDITIONS

by

D. C. White

UDC 629.19.052.2 : 551.465

ROYAL AIRCRAFT ESTABLISHMENT

Technical Report 82059

Received for printing 25 May 1982

THE ACCURACY OF SEASAT 1 ALTIMETER ALTITUDE MEASUREMENTS UNDER VARIOUS SEA STATE CONDITIONS

by

G. C. White

SUMMARY

This Report determines the accuracy with which the Seasat 1 altimeter height measurement can be used to derive the spacecraft CG to mean sea level distance. To calculate this accuracy a description of the mean shape of a reflected pulse must be used which incorporates a realistic description of a wavefield's waveheight probability distribution in its derivation. A quantitative description of such a reflected pulse is developed here. This description is then used in a simulation procedure to calculate values of the rms errors in the tracking and wave biases, hence the rms height error. This figure of accuracy, *ie* rms height error is derived for various sea state conditions.

Departmental Reference: Space 616

LIST OF CONTENTS

1 INTRODUCTION

The Seasat 1 satellite launched in May 1978 was the first satellite devoted to observation of the World's oceans. To perform this task one passive and three active microwave instruments were carried onboard this satellite. These instruments consisted of a synthetic aperture radar used for producing two-dimensional images of the ocean surface, a scanning multichannel microwave radiometer from which sea surface temperature, wind speed and atmospheric water vapour concentration could be derived and a scatterometer and altimeter. The scatterometer was basically a radar system used to measure the sea surface wind vector while the altimeter measured the rms waveheight of those waves lying in a region of sea directly beneath the satellite and the satellite's height above the sea surface.

With this instrument complement, the sea state variables of rms waveheight and dominant wavelength and direction were measured along with the meteorologically significant variable of the sea surface wind vector in all weathers.

One further instrument was carried - a visual and infra-red radiometer - which gave information about the prevailing weather conditions in the field of view of the four microwave instruments.

This Report is concerned with the altimeter instrument. As mentioned above this instrument measured the rms waveheight and satellite altitude. To derive the altitude the transit time of a very short duration pulse was measured. From this transit time measurement the distance between the mean sea level and the satellite's CG (centre of gravity) can be calculated. Combining this distance with the geocentric distance of the satellite the distance corresponding to the sum of the geoid and instantaneous sea surface height can be found. This quantity is of considerable interest to oceanographers and geodesists. By determining this sum both spatially over the oceans and in time, oceanographic features such as mesoscale eddies, ocean tides and currents can be measured. Included in the latter are the currents due to the large scale ocean circulation patterns. This circulation is responsible for heat transport from the tropics to the poles - consequently it has an effect on the climate. Currents can be measured by an altimeter since a current introduces a slope into a sea surface. This slope can be detected by measuring the change in the above sum along the spacecraft's ground track. Unfortunately the gradient of this slope is very small - typically only a few centimetres of height variation occurs over a horizontal distance of a hundred kilometres. Consequently the accuracy to which the satellite's altitude can be found must be as high as possible if such a small slope is to be detected.

To derive the satellite's altitude a series of corrections must be applied. These corrections are known as the instrumental and geophysical corrections. The instrumental corrections basically translate the satellite reference to the satellite CG while the geophysical corrections correct for the propagation delay introduced by the ionosphere and troposphere.

In this Report it is assumed that the instrument and geophysical corrections necessary to correct the measurement of altitude made by the Seasat 1 altimeter have been

applied[1]. The instrument corrections are accurately known and the uncertainty in the geophysical corrections is less than a few centimetres, provided that radiometer data is available to determine the magnitude of the wet component part of the tropospheric correction to the measured altitude. The error sources to be investigated here are due to tracking, discriminator and wave-bias noise. They arise due to the presence of noise on a pulse received after reflection by a sea surface and to the error this noise introduces into the values of the rms waveheight and skewness variables. Their magnitudes are obtained by fitting a theoretical description of the mean shape of a received pulse envelope to that obtained in practice.

To determine the accuracy of the Seasat 1 altimeter altitude measurements under varying sea state conditions (a range of rms waveheight and skewness values), a realistic description of the mean shape of a received pulse envelope (hereafter known as a mean waveform) must be developed. The theoretical basis of such a description is discussed in the first section of this Report along with a review of how the Seasat 1 altimeter measured the spacecraft's altitude by tracking to a specific point on a mean waveform's leading edge. The remainder of the Report is concerned with using this theoretical description of the mean waveform to determine the wave and tracking-bias errors and in conjunction with tracking error, the accuracy of an altitude measurement made by this altimeter.

2 ALTIMETER DESIGN AND OPERATION

2.1 General

Up to the end of 1980 only three spacecraft had included an altimeter within their instrument complement. These spacecraft were Skylab - the first American manned space laboratory, GEOS 3 a satellite used for geophysical research, and Seasat I, the first satellite devoted primarily to oceanographic remote sensing. Of these three altimeters, the one carried by Seasat 1 measured the altitude with the lowest level of instrumental range noise (10 cm as opposed to around 50 cm for the altimeter on GEOS 3 and approximately 1 m for the Skylab altimeter). To determine the accuracy in the measurement of the distance between the spacecraft CG and mean sea level, derived from a Seasat 1 altimeter, height measurement, an understanding of how this altimeter measured the satellite's altitude is needed. The design and operation of this altimeter will therefore be described.

2.2 The Seasat 1 altimeter

The design of this altimeter is illustrated schematically in Fig 1 and its parameters are given in Table 1.

To operate successfully this system has first to acquire the backscattered signal in the acquisition mode and then remain locked onto it in the tracking mode. In the acquisition mode an initial measurement of the transit time of a pulse is made. Owing to the low orbital eccentricity ($e < 10^{-3}$) of Seasat 1 the altitude only varied between ±40 km centred on 800 km. Consequently the transit time falls within the range 5.06 to 5.6 ms. To measure this time a monochromatic pulse of duration 3.2 μs, frequency 13.5 GHz is transmitted. At the time of triggering this pulse a range counter within the

SACU (synchroniser, acquisition and control unit) counts down for a pre-selected time interval before triggering the production of a CW LO (local oscillator) pulse of frequency 13.0 GHz and duration 3.2 μs. After first stage mixing the resulting signal is detected and passed to a threshold detector within the SACU. If this threshold is exceeded the value of the pre-selected time interval is used to form a 'height word', *ie* a word holding the best estimate of the transit time at that point. This word is then given to the ATU (adaptive tracking unit) and the tracking mode initiated. However, if the threshold is not exceeded, further monochromatic pulses are transmitted with the range counter counting down through a series of pre-determined time intervals until the threshold is exceeded and acquisition attained.

The tracking mode differs fundamentally from the acquisition mode owing to its use of the pulse compression technique. The principle advantage of this technique lies in its reduction of the peak transmitted power for the attainment of a specific SNR (signal-to-noise ratio) by eliminating the need for very short (~ns) duration pulses. As knowledge of this technique is essential for understanding the operation of the altimeter in the tracking mode the pulse compression technique will now be discussed.

2.3 The pulse compression technique

In this technique a chirped pulse, *ie* a pulse whose carrier frequency is swept linearly from 13.5 to 13.82 GHz in 3.2 μs (in the case of Seasat I) is employed. Considering only reflection by one point on a surface distance H from the altimeter (point B in Fig 2), then 2 H/C seconds after transmission of the pulse leading edge, the leading edge of the reflected pulse is received. On mixing this received pulse with a LO FM (frequency modulated) pulse whose frequency sweep rate equals that of the transmitted pulse but whose starting frequency is 13 GHz, a constant difference frequency F (equal to 500 MHz in the case of Seasat 1) for a specific height H will be observed. If H varies F will vary. Employing this procedure, all points at the same range will produce mixer outputs at the same frequency. Consequently integrating the power from the mixer at a particular frequency will give the total power backscattered and received by the altimeter's antenna from those points on a sea surface at the same range.

Onboard the spacecraft the received signal is sampled by a set of 60 contiguous filters which comprise the DFB (digital filter bank). The swept frequency rate is 100 MHz/μs and the time resolution of the system is 3.125 ns. The filter* bandwidth must be $\leq 100 \times 3.125 \times 10^{-3}$ MHz (*ie* 312.5 kHz) so as not to degrade the system time resolution. By integrating the DFB outputs over contiguous frequency intervals, each of bandwidth 312.5 kHz, the response from successive concentric annuli on a flat sea surface is obtained. Plotting the received intensity as a function of time gives the received pulse power envelope. The resulting shape of this received pulse would be precisely the same if instead of a 3.2 μs chirped pulse a pulse of 3.125 ns duration were transmitted and the received pulse were sampled with a filter of width 3.125 ns. The production of such a short duration pulse is a great problem due to the peak power required to provide a useful SNR (signal-to-noise ratio). As a chirped pulse width is 1024 times greater

* Each filter is also known as a gate.

than a pulse of duration 3.125 ns its peak power can be 1/1024 of that of a 3.125 ns wide pulse to achieve the same SNR.

2.4 Tracking mode operation

When used in the tracking mode the transit time is determined by the ATU. In practice 50 successive DFB outputs are stored and averaged in the ATU. The ATU then combines these averaged gate values in one of five ways. The procedure is illustrated in Fig 3. Combining the gates together by this means forms a tracking gate. Five tracking gates can be produced by the ATU, each tracking gate consisting of an early, middle and late gate. For each tracking gate the widths of the early, middle and late gates are the same, the output of these gates being obtained by summing the outputs of adjacent gates in the DFB which lie in the early, middle or late gate time range. The number of DFB gates lying in this range depends on which of the five tracking gates is being synthesised. This summing process is carried out by an algorithm run on a small micro-computer in the ATU. A variety of tracking gates were used so that the magnitude of the attitude error correction to the altitude measurement was minimised.

For this system to measure the transit time to the mean sea surface the intensity of that point on a received waveform's leading edge corresponding to the return from the mean sea surface must be known. According to the model of Miller and Brown[2]* (where the waveheight pdf is normally distributed) which describes the mean waveform, this intensity equals the power level of a mean waveform curve at the origin of the time axis. This intensity shows a small variation with σ_w this being 0.443 for a normalised mean waveform[3]. (In practice the 60 DFB gate outputs summed to a constant value, this being achieved by the use of an AGC system. Consequently all calculations involving a mean waveform assume it to be normalised.)

The time offset between this level (whose normalised power level was 0.443) and the level corresponding to the mean sea surface was calculated using the Miller and Brown model, taking $Er = 0^o$ and the results tabulated as a function of σ_w, being stored in the altimeter's micro-computer. By measuring the gradient of the mean waveform's leading edge, by subtracting the late gate output from the early gate, σ_w could be determined and thus the necessary time offset derived by interpolation. Consequently the transit time could be corrected.

To track to any particular point on a mean waveform's leading edge a tracking law of the form:

$$I(\tau) = M(\tau) - \alpha L(\tau + W)$$

is used. Here M and L are the power outputs of the middle and late gates, τ the offset of the centre of the middle gate from the desired tracking location, and W is the width of the middle and late gates.

---

* In this model all time measurements are made with respect to the time of reception of the mean sea level contribution to a waveform.

In practice the device is tracking successfully when $I(\tau) = 0$. By employing variable gate widths the stability and sensitivity of the system is maximised[2]. The condition $I(\tau) = 0$ is attained as follows.

Having obtained a timing offset the ATU now tries to vary the sequencing time, *ie* time between triggering the DDL (digital delay line) for the production of the transmitted and LO chirped pulses so as to centre the point on a mean waveform's leading edge whose normalised intensity is 0.443 in the DFB. The value of this sequencing time is expressed in the 17 MSB (most-significant-bits) of the 25 bit 'height word'. The value of these 17 MSB is used as the countdown time by the DDG (digital delay generator) which triggers the DDL. The value attributable to the 8 LSB (least-significant-bits) of this height word is used to vary the centre frequency of the individual gates of the DFB by the same amount so as to decrease the timing offset. This height word is formed for every received pulse, its value being derived from the previous height word added to a value from a feedback loop.

The feedback loop[3] is also part of the ATU. It produces a timing offset by taking the average offset for the previous 50 pulse grouping and adds a certain fraction of the timing offset to a rate accumulator and another fraction to a position accumulator. The sum obtained from these accumulators at millisecond intervals then provides the input to form a new height word. By constantly centring the DFB on the pulse leading edge, *ie* fine tuning, and varying the sequencing time, *ie* coarse tuning, the height word is continually updated and the device tracks smoothly. In this way the tracking condition $I(\tau) = 0$ is obtained.

This updating is needed because of an altitude rate or acceleration. When travelling over the sea the altitude rate varied smoothly, this variation being due mainly to orbital eccentricity. Over land this rate was often non-linear due to the presence of underlying rough terrain.

The DDG is contained within the SACU and as mentioned above triggers the production of a chirped pulse. The chirped pulses produced for transmission and mixing differ in their power level and frequency. Initially a chirped pulse centred on 250 MHz whose frequency is decreasing linearly in time is produced by applying a 12.5 ns pulse of centre frequency 250 MHz to a surface acoustic wave device. The resulting chirped pulse has a bandwidth of 80 MHz and a sweep rate of 3.2 μs. The bandwidth of this pulse is then increased by a factor of four. For transmission the centre frequency of this chirped pulse is up-converted to 3375 MHz and then multiplied by 4, resulting in a 13.5 GHz chirped pulse. For the LO chirped pulse the associated frequencies are 3250 MHz and 13 GHz.

In practice when lock, *ie* $I(\tau) = 0$ has been obtained the reflected and LO chirped pulses are combined in the first mixer. An output centred at 500 MHz is produced. Further mixing then occurs, with a CW oscillation of frequency 500 MHz. From this mixer two signals are obtained, the in-phase I and quadrature Q outputs (Q is the same as I except for a phase change of 90°). Both these signals are then sampled by a HSWS (high speed wave sampler) which undertakes analogue-to-digital conversion at a rate of 20 MHz, 64 samples being taken at equal intervals during 3.2 μs.

To complete the system, filtering by the DFB takes place in those intervals between successive pulse receptions. For an irradiated sea surface, contributions to the received waveform arise from various ranges. As each range is associated with a particular frequency the received waveform is synthesised from components covering a range of frequencies. To determine a waveform the power within each gate must be determined at each sampling time. Integration over a period of 3.2 μs for all the gates will give the waveform. This waveform is then taken by the ATU and used in the tracking process.

Apart from performing this tracking operation the ATU also provides information on the rms waveheight, the spacecraft's altitude, the AGC gain value and the waveform shape. The average of approximately 100 consecutive measurements of rms waveheight, AGC value and altitude were telemetered to ground along with the average of 100 consecutive waveform shapes.

3 QUANTITATIVE DESCRIPTION OF A MEAN WAVEFORM

3.1 General

This description will be developed as follows. Firstly the flat sea impulse response will be derived. This response is a description of the waveform received when a pulse of zero time duration has been scattered by a flat sea surface. The advantage of employing an impulse response to characterise a surface lies in its use in determining the mean waveform for rough sea surfaces which are illuminated by pulses of finite duration. For example if $P_s(\tau)$ describes the transmitted pulse shape as a function of time and $W(\tau)$ describes the distribution of surface elevations from a mean level, then the mean waveform P is obtained by evaluating the expression $I_r(\tau) * P_s(\tau) * W(\tau)$ [4,5] where $I_r(\tau)$ is the flat sea impulse response and $*$ denotes a convolution process.

To derive the flat sea response the assumption is made that the mean power levels received from elements of a scattering surface each having unit area are incoherent, so the powers sum linearly. This assumption is examined in section 3.2. To derive the mean power received per unit area of backscattering surface, $\underline{E}_s$ the scattered far field electric vector must be determined. $\underline{E}_s$ itself is produced by a surface current density $\underline{J}$ that has been induced in the sea surface by $\underline{H}$ (the magnetic field vector) of an incident electromagnetic (EM) wave.

3.2 Determination of the scattered far field electric vector and backscatter coefficient

In determining $\underline{E}_s$ an important criterion is whether the ratio R, between the characteristic scale size and EM wavelength, quantified by Barrick[6] as $2\pi h(x,y)/\lambda_i$ is greater than unity. Here $h(x,y)$ is the height of point (x,y) on the sea surface above mean sea level and λ_i is the wavelength of the impinging radiation. This ratio is important as the method of deriving $\underline{E}_s$ differs for the two cases. The two physical situations are illustrated in Fig 4. The top diagram shows the case $R > 1$. Here the surface is smoothly varying on a scale comparable with the wavelength. If visible light for example is incident in the direction shown and the backscattered component is viewed then the bulk of the reflected radiation will be seen to come from a series of small surface elements, the reflection being specular, *ie* mirror-like. This situation is well illustrated by the glinting phenomena seen when sunlight is reflected by a water surface.

In the region of these elements - so called 'specular points' the surface electric current density induced by the impinging EM field must be producing a scattered electric field component, the phase of which is only varying slowly across such a region resulting in constructive interference. For this to be so the surface would be expected to be normal to the impinging wave. Further from these regions, due to the tilt of the water surface, the phase variation between adjacent scattered components is much greater, so they tend to cancel. This picture is the same for microwave radiation with wavelengths of the order of centimetres incident on a smoothly varying surface of scale size greater than tens of centimetres.

The scattered electric field component E_s can be solved by the use of an integral expression[7] derived directly from Maxwell's equations. This takes the form:

$$\underline{E}_s = - i \frac{\omega\mu}{4\pi r} \int (\underline{I} - \underline{k}_s\underline{k}_s) \cdot \underline{J}(cr') \exp(ikr - i\underline{k}s \cdot \underline{r}')ds'$$

where ω is the angular frequency, k the wave number of the impinging EM wave and $\underline{k}_s$ the wave number vector of the scattered wave. $\underline{I}$ is the unit dyad and $\underline{J}$ the surface current density. The integral is evaluated over the actual scattering surface, all primed symbols being measured on this surface.

To determine $\underline{E}_s$ a description of $\underline{J}$ on the surface must be provided. At a frequency of 13.5 GHz seawater is a good conductor. Consequently the displacement current $\underline{D}$ is much smaller than the conduction current, so from Maxwell's equations linking $\underline{H}$, $\underline{J}$ and $\partial\underline{D}/\partial t$, $\underline{\nabla} \wedge \underline{H} = \underline{J}$ to a good approximation. Adopting a coordinate system defined by the three orthogonal unit vectors $\underline{\alpha}$, $\underline{\beta}$ and $\underline{\gamma}$ where $\underline{\alpha}$ and $\underline{\beta}$ lie on the plane of the mean surface and $\underline{\gamma}$ is anti-parallel to $\underline{k}$ and taking $\underline{H} = \underline{\alpha}H$ then:

$$\underline{J} = \underline{\beta} \frac{\partial H}{\partial \gamma} - \underline{\gamma} \frac{\partial H}{\partial \beta} .$$

The current into the surface is of no interest as this cannot produce a detectable scattered $\underline{H}_s$ component as $\underline{H}_s$ is orthogonal to $\underline{J}$, consequently only the component of $\underline{J}$ parallel to the surface is of interest.

In practice the so-called optical distribution is taken for $\underline{J}$ where $\underline{J} = 2\underline{\hat{n}} \wedge \underline{H}_i$. Here $\underline{\hat{n}}$ is the unit vector normal to the surface and $\underline{H}_i$ the magnetic field vector of the incident EM wave. In practice this form of $\underline{J}$ is somewhat unrealistic. For example if a sea surface as illustrated in Fig 5 is illuminated as shown, regions of the surface labelled 'a' are not illuminated, thus $\underline{J}$ here must be zero. One problem is what happens to the distribution of $\underline{J}$ at the edges of the illuminated regions. The abrupt discontinuities as implied by this optical distribution will not occur as the conduction current will be expected to flow out into the non-illuminated region, becoming dissipated by Joule heating and radiation. Secondly if deviations from the mean surface occur and the radiation impinges at low angles of incidence multiple scattering, *ie* scattering of a part of the incident wave that has already been scattered, will take place with increasing regularity (Fig 5).

The two points mentioned above will complicate the distribution of $\underline{J}$. No description of $\underline{J}$ has yet been developed which takes these two effects into account.

Normally altimeters illuminate the sea surface such that the angle of incidence to the mean surface is 90°. Consequently little obscuration and multiple scattering is likely to occur - except in the case of highly agitated seas where the waves are breaking. Such sea conditions occur infrequently as they are associated with severe storms.

The picture is further complicated as a sea surface is composed of features ranging from scale sizes of centimetres to hundreds of metres. Such scale sizes can cause R to be less than and greater than unity at different points on the surface. Having both roughness scales on a sea surface produces an example of what is known in the literature as a composite surface. The presence of small scale structure (R < 1 case, Fig 4) produces diffraction at the surface - this complicates the theoretical treatment as to evaluate the scattering integral the induced surface current density and the shape of the surface must be known precisely.

The problem of scattering by composite surfaces has been examined by a number of authors (see Ref 8 and references therein) with the mathematical technique of Burrows[9] used by Brown[10] being the most satisfactory to date as it derives σ^* for all angles of incidence rather than just for large and small angles of incidence as other techniques have. The essential result of Brown's work is that for angles of incidence $<5^{\circ}$ the contribution to σ due to diffraction is under 2% of that of large scale (R > 1) scatter. This diffraction contribution to specular scatter will be ignored here.

As mentioned previously the bulk of the scattered radiation comes from a large number of physically separate elements - the specular points. To determine the value of $\underline{E}_s$ at distance $\underline{r}$ from a scattering surface one needs to sum over the contributions of each of the components. As shown by Kodis[7] the contribution E_{js} to $\underline{E}_s$ by one specular point for an incident electric field of unit amplitude is given by:

$$E_{js} = \frac{ik}{4\pi} \frac{\underline{F}_j}{\hat{\underline{n}}_j \cdot \hat{\underline{e}}_z} e^{ikr} \int_s \exp ik(\underline{q} \cdot \underline{r}) dydx$$

where $\underline{F}_j = (\underline{I} - \underline{k}_s\underline{k}_s) \cdot (\underline{k} \wedge \hat{\underline{n}}_j)$, $\underline{q} = \underline{k}_i - \underline{k}_s$, $\underline{k} = \underline{k}_i \wedge \hat{\underline{e}}$ and $\hat{\underline{n}}_j \cdot \hat{\underline{e}}_z = dxdy/ds_j$. Here (x,y) is the mean level plane of the surface, z lying orthogonal to (x,y). This coordinate system is centred on the jth element. Further $\underline{k}_i$ and $\underline{k}_s$ are the incident and scattered wave number vectors. $\hat{\underline{n}}_j$ is the unit normal vector of the jth element, $\hat{\underline{e}}$ is the unit vector of the incident $\underline{E}_i$ field ($\hat{\underline{e}}_z$ its z component). The integral is evaluated over that portion of the level plane corresponding to the projection of the elemental surface onto this plane. To evaluate this integral the method of stationary phase[11] can be used if k is large.

---

* σ is the backscatter cross section for a unit area of scattering surface. σ is defined by the relationship $\sigma = 4\pi r^2 \langle E_s^2 \rangle / \langle E_i^2 \rangle$ where E_s is the scattered electric field intensity derived for a unit area of the scattering surface at distance r from the surface and E_i is the incident electric field intensity seen by this unit area. σ is also known as the backscatter coefficient.

Using this method of integration the solution of E_{js} is:

$$E_{js} = \varepsilon_j (e^{ikr}/r)\underline{F}_j / q \cdot (\hat{\underline{n}}_j \cdot \hat{\underline{e}}_z) \exp ik(\underline{q} \cdot \underline{r}_j) \left| A_j C_j - B_j^2 \right|^{-\frac{1}{2}}$$

where ε_j = +1 at a relative maximum, and $A_j = \partial^2 k_j / \partial x^2$,*
-1 at a relative minimum, $B_j = \partial^2 k_j / \partial x \partial y$,
+i at a saddle point, $C_j = \partial^2 k_j / \partial y^2$.

To determine the total scattering field E_s, the contributions from each scattering element are summed. Consequently:

$$\left\langle E_s^2 \right\rangle = |F|^2 / q^2 r^2 (\cos \theta_z)^4 \left\langle \sum_{j,k} |D_j D_k|^{-\frac{1}{2}} \exp(i\underline{k}_q \cdot (\underline{r}_j - \underline{r}_k)) \right\rangle$$

where $\cos \theta_z = \hat{\underline{q}} \cdot \hat{\underline{e}}_z$ as $F_j / \hat{\underline{n}}_j \cdot \hat{\underline{e}}_z = F / \hat{\underline{q}} \cdot \hat{\underline{e}}_z$ and $D_j = |A_j C_j - B_j^2|$.

Since

$$\sigma = 4\pi r^2 \left\langle E_s^2 \right\rangle$$

then

$$\sigma = 4\pi |F|^2 / q^2 (\cos \theta_z)^4 \left\langle \sum_{j,k} |D_j D_k|^{-\frac{1}{2}} \exp(i\underline{k}_q \cdot (\underline{r}_j - \underline{r}_k)) \right\rangle .$$

Assuming the phase to be random between each of the scatterers, *ie* each scatters independently of the others. This is reasonable as the phase dispersion introduced by a rough scattering surface is large as the characteristic scale size $\gg \lambda_i$ in most cases, and over a large number of scattering elements the cross terms will sum to zero. Thus:

$$\sigma = 4\pi |F|^2 / q^2 \cos^4 \theta_z \left\langle \sum_{j,k} |D_j D_k|^{-\frac{1}{2}} \right\rangle .$$

Expressing this in terms of the two principal radii of curvature at each point, the radar cross section becomes

$$\sigma \approx \pi \left\langle \sum_{j,k} \left| (R_a R_b)_j (R_a R_b)_k \right|^{\frac{1}{2}} \right\rangle$$

82059

* k_j is the elevation of point j above the mean level plane.

where $R_a/R_b = 1/K$, and $D_j \cos^2\theta_z = K_j|(\partial r/\partial x) \wedge (\partial r/\partial y)|^2$, K_j being the Gaussian curvature at point j.

Taking the ensemble average:

$$\sigma \approx \pi\overline{R_a R_b}\langle N\rangle$$

where N is the average number of specular points per unit area. Finally introducing $F(\eta)$ the Fresnel reflection coefficient, then

$$\sigma = \left\langle |F_j(\eta)|^2 \right\rangle \pi\overline{R_a R_b}\langle N\rangle \quad ,$$

η being the angle of incidence to the surface for each point j.

To be of practical use $\overline{R_a R_b}$ and $\langle N\rangle$ must be re-expressed in terms of more easily observable quantities. Work by Barrick[12] has shown that these factors can be replaced by the expression $\sec^4\gamma p(\Delta x,\Delta y)$ to a good order of approximation. Here γ is the angle between the normal to the level plane of the surface and the local surface normal at the scattering point. For backscatter γ equals the angle of incidence. The expression $p(\Delta x,\Delta y)$ is the joint slope probability distribution, where Δx and Δy are the surface slopes measured in orthogonal directions within the surface at some point. The expression for σ now becomes:

$$\sigma = \pi\left\langle |F_j(\eta)|^2 \right\rangle \sec^4\gamma p(\Delta x,\Delta y) \quad .$$

This expression can be used to determine the mean waveform. In using this expression within the illuminated area the wavefield will be assumed to be homogeneous. As σ is a statistical parameter owing to its dependence on $p(\Delta x,\Delta y)$ the resulting waveform has an averaged form. Finally as $\sigma = \int\sigma(z)dz$, z being orthogonal to the plane of the mean surface then $\sigma(z)$ will take the form:

$$\left\langle |F_j(\eta)|^2 \right\rangle \pi \sec^4\gamma p(z;\Delta x,\Delta y) \quad .$$

A description of $p(z;\Delta x,\Delta y)$ must now be obtained.

3.3 Description of the joint height, slope probability density function

In past work $p(z;\Delta x,\Delta y)$ has been assumed to be normal. *In-situ* measurements of sea surface height elevations as a function of time have shown the wavheight pdf (probability density function) to have a skewed Gaussian form[13]. Consequently the joint height and slope pdf (hereafter known as wave joint pdf) will not be normal. In practice the crests and troughs of a rough sea surface are of unequal curvature. The troughs are far more rounded than the crests which often exhibit a marked degree of peakiness. If the waveheight pdf were normal the crests should be mirror images of the troughs. To explain this observed skewness in the waveheight pdf non-linear interactions between the wave motions interacting to produce a sea surface are invoked.

Longuet-Higgins[14] has derived the form of $p(z;\Delta x,\Delta y)$ for a long crested sea (here the cross section of a sea surface is taken to be dependent on x and z only, consequently $\Delta y = 0$) and finds that:

$$p(z;\Delta x) = \left(2\pi\sigma_z^2\sigma_{\Delta x}^2\right)^{-\frac{1}{2}}\left\{1 + (\lambda/6)\left((z/\sigma_z)^3 - 3z/\sigma_z\right) + (\lambda_1 z/2\sigma_z)\left((\Delta x/\sigma_{\Delta x})^2 - 1\right)\right\} \times \exp\left(-\tfrac{1}{2}\left((z/\sigma_z^2) + (\Delta x/\sigma_{\Delta x})^2\right)\right) .$$

Here, σ_z and $\sigma_{\Delta x}$ are the standard deviations of the surface elevations and slopes and λ and λ_1 the skewness coefficients defined by:

$$\lambda = \mu_{30}/\sigma_z^3 , \qquad \lambda_1 = \mu_{12}/\sigma_z\mu_{02}$$

where μ_{mn} is a moment of the distribution $p(z;\Delta x)$ given by $\langle z^m \Delta x^n \rangle$.

Jackson[15] has used the results of Longuet-Higgins with the assumption of a fully developed sea* to show that $\lambda_1 = 2\lambda$. For radiation to be received back at the altimeter $\theta \lesssim 0.5^\circ$ consequently only the backscatter component is of interest in altimetry, thus $\Delta x = \Delta y = 0$ to a good approximation. So

$$p(z;0) = \left(2\pi\sigma_z^2\right)^{-\frac{1}{2}}\left(1 + (\lambda/6)\left((z/\sigma_z)^3 - 9z/\sigma_z\right)\right)\exp\left(-z^2/2\sigma_z^2\right) .$$

Therefore the final form for $\sigma(z)$ is:

$$\left\langle |F_j(0)|^2 \right\rangle \pi p(z;0) , \qquad \text{as } \sec^2\gamma = 1 \text{ and } \eta = 0 .$$

$$= \sigma_0\left(2\pi\sigma_z^2\right)^{-\frac{1}{2}}\left(1 + (\lambda/6)\left((z/\sigma_z)^3 - 9z/\sigma_z\right)\right)\exp\left(-z^2/2\sigma_z^2\right) .$$

This above pdf has its mean located at $z = -\lambda\sigma_z$[15] , while the mean for a normally distributed pdf is at 0 m. This difference in the position of the mean is known as the wave-bias.

3.4 Derivation of the flat sea impulse response

Fig 6 illustrates the geometry associated with the reflection of a pulse of infinitesimal duration (strictly a mathematical abstraction produced for theoretical convenience) by a flat sea surface. OA is the boresight axis of the altimeter, *ie* the axis along which the gain of the altimeter's antenna is a maximum, OB the axis along which power contributed by element B arrives and E_r is the attitude error angle. Taking the power output of the altimeter transmitter as P watts, the gain of the antenna as G then the effective radiated power is PG watts. Finally the pulse is transmitted at time

* A fully developed or aroused sea is one whose energy spectrum has attained equilibrium. Physically this means that a balance has been reached between the energy passed into the waves by the wind to that lost when the waves break.

zero. In deriving this response the method used here is a simplification of that used by Brown[16].

At B the power received per unit area will be $PG/4\pi R_1^2$, the power reflected back from an area dA at B being $PG\sigma dA/4\pi R_1^2$. Thus the power per unit area received back at the altimeter will be $PG\sigma dA/4\pi R_1^2 \times 1/4\pi R_1^2$. For an aerial of gain G, working at a wavelength λ, the effective area is $G\lambda^2/4\pi$. Consequently the power received through the aerial is $PG/4\pi R_1^2 \times G\lambda^2/4\pi \times \sigma dA/4\pi R_1^2$.

For such an infinitesimal pulse being reflected from a flat sea surface, the region of the sea illuminated is initially just a point which then becomes a ring of infinitesimal width and increasing diameter. The area of such a ring is $\rho d\phi$. If the distance of the points of a ring from the altimeter is R_1 (Fig 6), then power is received from the ring $2R_1/c$ seconds after the pulse is transmitted. Consequently the power P(t) received from the ring at time t is:

$$P(t) = \int_{\phi} \delta(t - 2R_1/c)\left(PG^2\sigma\lambda^2/R_1^4(4\pi)^3\right)\rho d\phi$$

where $\delta(t - 2R_1/c)$ sets the time of reception, since $\delta(t - 2R_1/c)$ is unity if $t = 2R_1/c$ and zero otherwise. From the geometry,

$$R_1^4 = H^4\left(1 + (\rho/H)^2\right)^2 .$$

The gain of the aerial is given by

$$G(\theta) = G_0 \exp(-2 \sin \theta/\gamma)$$

where θ is the angle between the boresight axis and the OB axis in Fig 6. For a flat sea and small attitude error (<0.5) σ is virtually constant. Setting $\sigma = \sigma_0$ to denote this and substituting $K = \rho/H$ then

$$P(t) = \frac{\lambda^2 G_0^2}{(4\pi)^3 H^4} \int_{\phi} \frac{\delta(t - 2R_1/c) \exp\{-4 \sin^2\theta/\gamma\}}{(1 + K^2)^{\frac{1}{2}}} \rho d\phi .$$

Before this integral can be evaluated the functional dependence between θ, ρ and ϕ must be established. From Fig 6:

$$AB^2 = \rho^2 + H^2 \tan^2 E_R - 2\rho H \tan E_R \cos \phi .$$

As

$$AB^2 = R_1^2 + R_2^2 - 2R_1R_2 \cos \theta$$

also, then

$$\cos \theta = \left(R_1^2 + R_2^2 - \rho^2 - H^2 \tan^2 E_R + 2\rho H \tan E_R \cos \phi\right) \Big/ 2R_1R_2 .$$

But

$$R_2 = H \sec E_R \quad \text{and} \quad R_1^2 = H^2(1 + K^2)$$

and so

$$\cos\theta = \left(\cos E_R + K \sin E_R \cos\phi\right) \Big/ (1 + K^2)^{\frac{1}{2}} .$$

Hence the resulting integral is

$$P(t) = \frac{\lambda^2 G_0^2 \sigma_0}{(4\pi)^3 H^4} \int_\phi \frac{\delta(t - 2R_1/c) P \exp\{w\}}{(1 + K^2)^2} \rho d\phi$$

where

$$w = -\frac{4}{\gamma}\left\{1 - \frac{\left(\cos E_R + K \sin E_R \cos\phi\right)^2}{1 + K^2}\right\} .$$

This expression is known as the impulse response integral. As shown in Appendix A:

$$P(\tau) = \frac{2\pi\lambda^2 G_0^2 \sigma_0}{(4\pi)^3 H^4} \exp\left\{-\frac{4}{\gamma}\sin^2 E_R\right\} \exp\left\{-\frac{4c\tau}{\gamma H}\cos^2 E_R\right\} \cdot (1 + \alpha^2)$$

where $\alpha = 4c\tau \sin^2 2E_R / \gamma^2 H$.

This description is valid for $\tau \geq 0$. For $\tau < 0$, $P(\tau) = 0$.

3.5 Final convolution procedure

Having obtained the quantitative description of the impulse response three further convolutions must be performed before a quantitative description of a mean waveform $P(\tau)$ is obtained. Schematically $P(\tau)$ is given by

$$P(\tau) = I_r(\tau) * P_s(\tau) * W(\tau) * I_t(\tau) ,$$

where $I_r(\tau)$ is the flat sea impulse response, $P_s(\tau)$ is the pulse shape distribution, $W(\tau)$ is the waveheight pdf and $I_t(\tau)$ is the instrument transfer function. The symbol * denotes a convolution process. The order in which the above convolutions are carried out is not important on physical grounds, however mathematical simplicity does dictate an order. This is that firstly the convolution of P_s with W is performed, this produces a function R . Then R is convolved with I producing a function S and lastly S is convolved with I_r giving P . The formation of R is given in Appendix B, that of S and P in Appendix C.

Two points must be noted. In approaching a roughened sea surface, surface elevations represented by the tail on the positive side of the time axis of a waveheight pdf will be encountered first by an impinging altimeter pulse. As the convolution process causes a function to be reversed before integration proceeds, for P to portray the effect of an asymmetric pdf correctly the waveheight pdf must be reflected, *ie* reversed

about its probability axis before the convolution takes place. In Appendix C this is done by multiplying the parameters F and G by minus one. Secondly the function describing P_s has been described by a normal distribution. Consequently it is symmetrical.

4 ACCURACY OF THE SEASAT 1 ALTIMETER HEIGHT MEASUREMENT

4.1 General

The Seasat 1 processed altimeter height data, *ie* the initial height measurement corrected for instrumental and ionospheric and tropospheric propagation delays is not a measurement of the true satellite altitude, *ie* distance from the spacecraft CG to mean sea level. Two further corrections, the tracking and wave-bias corrections have to be applied to the processed height values to derive true height values. Consequently the accuracy of the true altitude measurement depends on the accuracy with which each of these corrections is known, this accuracy being expressed in terms of a standard deviation in the two corrections.

The ideal tracking situation would be for the ATU to automatically track to that point on the leading edge of a waveform hereafter known as the mean sea point whose associated power level P corresponds to the contribution of those specular points (facets) being at mean sea level. Unfortunately the time ordinate of this point varies with the prevailing sea state conditions (σ_w and λ)* and the attitude error angle E_R. So without knowledge of these three variables it cannot be tracked. In setting up the altimeter on Seasat 1 the variables λ and E_R were taken to be zero and by using AGC to keep the mean integrated power per 100 consecutively received pulses constant the point on the leading edge of a mean waveform whose normalised power level was 0.443 was tracked. The processed height measurements were corrected during ground based processing for the effect of $E_R \neq 0^o$ but λ was always assumed to be zero as the waveheight pdf was always assumed to be normal.

The work presented here although similar to that carried out by Hayne[17] was developed independently. The derivation of the quantitative description of a mean waveform is presented here in greater detail than in the published work of Hayne. Further a description of the discriminator curve is also given.

If the ATU is arranged to track the mean sea point for a particular value of σ_w where $E_R = 0^o$ and $\lambda = 0^o$ then for other values of σ_w or either $E_R \neq 0^o$ or $\lambda \neq 0$ for the same σ_w value a different point will be tracked. In each case the time separation between the point tracked and the mean sea point must be calculated. This distance equals the sum of the tracking and wave-bias corrections.

4.2 Tracking and wave-bias corrections

As mentioned in section 2.4 the tracking law employed by the ATU is of the form $I(\tau) = M(\tau) - \alpha L(\tau + W)$ $I(\tau)$ is the output of the tracking gate for time offset τ, τ being the displacement of the centre of the middle gate M from the origin of the time axis of the waveform. L is the late gate output, W the width of the late gate and α a parameter which in conjunction with W dictates which point on the leading edge

* λ here denotes the waveheight pdf skewness variable.

is tracked. The distribution of I with τ is known as the discriminator curve and is obtained by convolving the waveform with the middle and late gate functions and then applying the expression for $I(\tau)$ given above. The deviation of the expression of a discriminator curve is discussed in Appendix D. Both the waveform and discriminator curve have coincident time origins. The tracking-bias is given by the value of τ when $I(\tau) = 0$, with the point on the waveform corresponding to $I(\tau) = 0$ being tracked. This bias value is dependent on the values of λ, σ_w, E_R, W and α.

The wave-bias correction arises due to the displacement of the mean of a skewed normal distribution compared to the mean of a normal distribution. If the waveheight pdf is represented by a normal distribution then the point on a waveform whose time ordinate is at the origin of the time axis is the mean sea point. For a waveheight pdf having a skewed form the time ordinate of the mean sea point will be $2\lambda\sigma_w/c$ seconds. This is the magnitude of the wave-bias correction.

4.3 Simulating the determination of σ_w and λ

To apply the tracking and wave-bias corrections λ, σ_w and E_R must be known. E_R is calculated from knowledge of a spacecraft's pitch, roll and yaw angles as measured by the spacecraft's attitude stabilisation system. The values of λ and σ_w and their variances are obtained by a least squares fit in these parameters to mean waveform data. To answer the question as to the accuracy of a true height value obtained from processing Seasat 1 altimeter data this fitting process was simulated to provide values of the standard deviation of the tracking and wave-bias corrections.

Examination of the form of a mean waveform's quantitative description given in Appendix C shows that is is non-linear in the variables λ and σ_w. Consequently this necessitates use of the differential least squares procedure so that the normal equations developed in this method are linearised, *ie* only linear terms in λ and σ_w are produced. However use of the differential least squares method does not automatically guarantee that sensible or realistic values of the fitting variables will be determined as the procedure is iterative and can thus diverge. Although only σ_w and λ are of interest, to fit the theoretical waveform to modelled waveforms a third variable T (time displacement) must be introduced as the origin of the modelled waveform's time axis is not known. If uncertainty occurs in the integrated power level a fourth variable, power gain must be fitted for. Adopting this method a matrix equation of the form $\tilde{\tilde{D}}\tilde{X} = \tilde{R}$ results, where

$$\tilde{\tilde{D}} = \begin{pmatrix} \sum\left(\frac{\partial f}{\partial \sigma_w}\right)^2 & \sum \frac{\partial f}{\partial \sigma_w}\frac{\partial f}{\partial \lambda} & \sum \frac{\partial f}{\partial \sigma_w}\frac{\partial f}{\partial T} \\ \sum \frac{\partial f}{\partial \lambda}\frac{\partial f}{\partial \sigma_w} & \sum\left(\frac{\partial f}{\partial \lambda}\right)^2 & \sum \frac{\partial f}{\partial \lambda}\frac{\partial f}{\partial T} \\ \sum \frac{\partial f}{\partial T}\frac{\partial f}{\partial \sigma_w} & \sum \frac{\partial f}{\partial T}\frac{\partial f}{\partial \lambda} & \sum\left(\frac{\partial f}{\partial T}\right)^2 \end{pmatrix},$$

$$\tilde{X} = \begin{pmatrix} \Delta\sigma_w \\ \Delta\lambda \\ \Delta T \end{pmatrix} \quad \text{and} \quad \tilde{R} = -\begin{pmatrix} \sum r \frac{\partial f}{\partial \sigma_w} \\ \sum r \frac{\partial f}{\partial \lambda} \\ \sum r \frac{\partial f}{\partial T} \end{pmatrix} .$$

f is the function describing the theoretical waveform and $\partial f/\partial\sigma_w$, $\partial f/\partial T$ and $\partial f/\partial\lambda$ the derivatives at points i, $i = 1, 60$ ($i = 1$ corresponds to gate -30, $i = 60$ to gate +30 of the DFB of the Seasat 1 altimeter system). $\Delta\sigma_w$, $\Delta\lambda$ and ΔT are increments in the guess values of σ_w, λ and T to be solved for, and r are the residuals.

To determine the standard deviation and correlation between the fitted variables a covariance matrix was introduced. As

$$\tilde{D}\tilde{X} = \tilde{R}$$

then

$$\tilde{D}^{-1}\tilde{D}\tilde{X} = \tilde{D}^{-1}\tilde{R} .$$

Consequently $\tilde{X} = (\tilde{D}^{-1}\tilde{D})^{-1}\tilde{D}^{-1}\tilde{R}$, the covariance matrix $\tilde{C}$ being $(\tilde{D}^{-1}\tilde{D})^{-1}$. Having found the values of σ_w, λ and T the variance of each of these terms is found by first calculating the variance of the residuals V_r, *ie* using the above σ_w, λ and T values in the theoretical description and determining the residuals between the predictions of this description and the modelled data.

Writing $\tilde{C}$ as

$$\begin{pmatrix} a_{11} & a_{12} & a_{13} \\ a_{21} & a_{22} & a_{23} \\ a_{31} & a_{32} & a_{33} \end{pmatrix}$$

then the variance of $\Delta\sigma_w$ is $V_r a_{11}$, of $\Delta\lambda$ is $V_r a_{22}$, and of ΔT is $V_r a_{33}$. The correlation coefficient between $\Delta\sigma_w$ and $\Delta\lambda$ is $a_{12}/\sqrt{a_{11}a_{22}}$, between $\Delta\sigma_w$ and ΔT is $a_{13}/\sqrt{a_{11}a_{33}}$ and between $\Delta\lambda$ and ΔT is $a_{23}/\sqrt{a_{22}a_{33}}$.

To start the fitting procedure initial guess values had to be provided. Initially no noise was added to the modelled waveform but even in this case the method diverged - the normal equations were virtually multiples of one another as the determinant derived in producing the inverse of $\tilde{D}^{-1}\tilde{D}$ became singular after a few iterations. Only in the case of σ_w, λ and T being very close to the values used in producing the noise-free waveform did the method converge and produce the correct values of σ_w, λ and T. To overcome this singularity difficulty a weighting matrix was introduced.

As $\tilde{D}\tilde{X} = \tilde{R}$, let $\tilde{W}$ be a weighting matrix then:

$$\tilde{W}\tilde{D}\tilde{X} = \tilde{W}\tilde{R}$$

and

$$\tilde{X} = (\tilde{D}^{-1}\tilde{W}\tilde{D})^{-1}\tilde{D}^{-1}\tilde{W}\tilde{R}$$

the covariance matrix $\tilde{C}$ now being $(\tilde{D}^{-1}\tilde{W}\tilde{D})^{-1} \cdot \tilde{W}$ is a diagonal matrix in this case having dimensions 3×3. After some initial experimentation it was found that provided $\Delta\sigma_w$ and $\Delta\lambda$ were highly weighted (implying little change in their value over successive iterations) compared to T convergence was possible. In practice the weighting factors applied to $\Delta\sigma_w$ and $\Delta\lambda$ were equal having the value 10^6, while the third weighting factor had a value of unity. Varying these values did not affect the value of the variances in $\Delta\sigma_w$, $\Delta\lambda$ and ΔT significantly provided the ratio of the weighting factors of $\Delta\sigma_w$ and $\Delta\lambda$ to ΔT were kept $\gtrsim 10^6$. As this ratio was reduced singularities were more likely to occur with the iterative process often diverging beforehand. Random noise was then added to a modelled waveform - as in practice waveforms are contaminated with noise. The independence of the variance of $\Delta\sigma_w$, $\Delta\lambda$ and ΔT with the weighting factor values was then verified. Further the values of $\Delta\sigma_w$, $\Delta\lambda$ and ΔT were all highly correlated owing to the use of such large weighting factor values applied to two of the variables. The values of the variances however were unrealistic as the variance on each of the variables was much smaller than the difference between the value of the variable used in deriving the model waveform and the value obtained from the fitting process. To derive more realistic values of the variances the following method was employed.

For specified values of σ_w, λ and T a modelled waveform was produced. Random noise was added to this waveform to attain a SNR of either 30, 20 or 10. Initial guess values were derived by adding random noise to the modelled waveform's values of σ_w, λ and T. For σ_w this guess value was within 10% of the model value, for λ within 50% and T within 100%. With these guess values, convergence was obtained after 10 to 15 iterations. This process was then repeated a further 99 times, using the same σ_w, λ and T values but using different initial guess values and adding new noise to the modelled waveform producing the same SNR as before. The result of this process was 100 σ_w, λ and T values. Having such a large data base enables reliable values of the variance in σ_w, λ and T to be calculated.

Having done this for one set of σ_w and λ values this procedure was repeated for further values of σ_w. Owing to the high correlation between $\Delta\sigma_w$ and $\Delta\lambda$ hence σ_w and λ, the tracking and wave-bias corrections will be highly correlated. Consequently the mean and variance of the wave-bias and tracking correction must be obtained by calculating the two corrections for each of the σ_w and λ values and then finding the mean and variance of the biases rather than finding the mean and variance of both σ_w and λ from the 100 values and then determining the mean and variance of the two biases. Similarly in calculating the mean of the wave-bias plus tracking correction, *ie* the offset correction, this correction must be determined for each σ_w and λ value and then the mean and variance calculated.

One further possibility remains, does the magnitude of the standard deviation of the offset correction vary significantly with λ for a constant value of σ_w and E_R ? To answer this question this standard deviation was calculated for $\lambda = 0$ and $E_R = 0^o$. The results obtained for the standard deviation for $\lambda = 0$ and 0.4 were similar (differing by only a few centimetres) to the results obtained for $\lambda = 0.2$. To provide estimates of the error bars on the points in a plot of rms waveheight versus standard deviation of the offset correction the results for SNR = 30 and 20 have been used to predict results at SNR = 10 - this being the mean SNR for Seasat 1 mean waveforms. For SNR = 30 the values of the standard deviation of the offset correction were multiplied by $\sqrt{3}$, for SNR = 20 by $\sqrt{2}$. The results for $\lambda = 0$, 0.2 and 0.4 with SNR = 10 were then used to derive mean values of the standard deviation of the offset correction and its standard deviation for various σ_w values.

4.4 Tracking error contribution

To determine the accuracy of the true height measurement one further error source must be considered - tracking error. This arises owing to the presence of noise on the received waveform. This noise causes an error in the positioning of the tracking gate, *ie* value of τ for the condition $I(\tau) = 0$. From the work of Brooks and Dooley[18] the standard deviation of this height error σ_R introduced by random noise is:

$$\sigma_R = N_p^{-\frac{1}{2}} \left\{ \frac{\sigma_w^2}{\alpha^2} \left(T_p + \frac{1}{a} \right)^2 \left(\frac{\Delta t'}{T_e} + \frac{\Delta t'}{T_i} \right) + \frac{T_e \Delta t}{12} \right\}^{\frac{1}{2}} \quad \text{metres,}$$

where a is the power SNR, T_e and T_i are the widths of the middle and late gates expressed in metres, $\Delta t'$ is the height resolution cell size, σ_w the rms waveheight, α is a constant of value 0.3327, T_p is the point tracked to, and N_p is the number of pulses averaged.

In this work T_p has been taken to be 0.5. $\Delta t = c_t$ where $t = 1$ ns , and $c = 3 \times 10^8$ metres. $T_e = T_i = \alpha_i c_t$ where α_i are the number of DFB gates combined to form the middle and late tracking gates and $N_p = 1000$. With these values:

$$\sigma_R = \left\{ \frac{10^3 \sigma_w^2}{(0.3327)^2} \left(\frac{0.5\ \text{SNR} + 1}{\text{SNR}} \right) \left(\frac{2}{\alpha_i} \right) + \frac{\alpha_i (ct)^2}{12} \right\}^{\frac{1}{2}} \quad \text{metres.}$$

The values of α_i for various values of σ_w are given in Table 2. The reason for these values is discussed in Appendix D.

4.5 Determination of the total error

Finally to arrive at the true height accuracy the variances of the offset correction and tracking error were added, the square root of the sum being taken to give a figure for the above accuracy. The assumption made here was that the offset correction and tracking error were statistically independent. Table 3 indicates the figures of accuracy expected for a variety of σ_w values with SNR = 10. These results are plotted in Fig 7.

This figure shows that the true altitudes in the case of the Seasat 1 altimeter can be calculated with an accuracy of better than 20 cm provided $\sigma_w < 5$ m. Consequently it is worth applying the total correction as the magnitude of this is greater than the magnitude of its standard deviation. However it must be remembered that Fig 7 has been obtained assuming that: (1) the transmitted pulse shape is normally distributed, (2) that the waveheight pdf used in the waveform derivation is valid for all sea state conditions, and (3) that the theoretical treatment of the backscattering problem used here is adequate. If the pulse shape of (1) were not normal, no effect on Fig 7 is to be expected. To verify points (2) and (3) further experimental work is required.

5 CONCLUSION

This Report has presented the development of a more realistic description of a mean waveform than those developed previously. Having done this the question - to what accuracy can the true altitude be calculated from Seasat 1 altimeter height measurements? has been answered. For the SNR applicable to this altimeter's mean waveforms it is found that the accuracy is better than 10 cm for $\sigma_w = 1$ m, while even for very rough seas ($\sigma_w \approx 5$ m) the accuracy is better than 20 cm.

Appendix A

EVALUATION OF THE IMPULSE RESPONSE INTEGRAL

In section 3.4 a quantitative description of the impulse response is desired. To obtain this an integral of the form

$$P(t) = \frac{\lambda^2 G_0^2 \sigma_0}{(4\pi)^3 H^4} \int_\rho \frac{\delta(t - 2R/c)\, \exp(W)}{(1 + K^2)^2}\, \rho d\phi$$

has to be evaluated. This Appendix is concerned with this evaluation. In the above expression:

$$W = -\frac{4}{\gamma}\left\{1 - \frac{(\cos E_R + K \sin E_R \cos \phi)^2}{1 + K^2}\right\}$$

$$= -\frac{4}{\gamma}\left\{1 - \frac{\cos^2 E_R}{1 + K^2}\right\} + \frac{4K \sin 2E_R \cos \phi}{\gamma(1 + K^2)} + \frac{4K^2 \sin^2 E_R \cos^2 \phi}{\gamma(1 + K^2)}$$

where $K = \rho/H$.

A point at distance R from the altimeter will return a contribution at time $t = 2R/c$ seconds after pulse transmission.

As $R = (H^2 + \rho^2)^{\frac{1}{2}}$ and $K = \rho/H$ then

$$K = \left(\frac{c^2 t^2 - 4H^2}{4H^2}\right)^{\frac{1}{2}} .$$

Translating the time origin such that time measurements are now made with respect to the time at which the mean sea level contribution is received, *ie* $\tau = t - 2H/c$, H being the distance between the spacecraft centre of gravity and the mean sea level, then $K = (c^2\tau^2 + 4H\tau c)^{\frac{1}{2}}/2H$. As $H = 8 \times 10^5$ m (Seasat 1 satellite) and $|\tau| \leq 100$ ns (width of Seasat 1 DFB dictates the time range in which a signal can be sampled) then $K = (c\tau/H)^{\frac{1}{2}}$ to a good order of approximation. Further $K/(1 + K^2) = (c\tau/H)^{\frac{1}{2}}$ and $K^2/(1 + K^2) = c\tau/H$. Consequently

$$P(\tau) = A \int_\phi \delta\left(\tau - \frac{2}{c}(R - H)\right)\left\{\exp \frac{4}{\gamma}\left(\frac{c\tau}{H}\right)^{\frac{1}{2}} \sin 2E_R \cos \phi\right\}$$

$$\times \exp\left\{\frac{4}{\gamma}\frac{c\tau}{H} \sin^2 E_R \cos^2 \phi\right\} \rho d\phi ,$$

where $A = \frac{\lambda^2 G_0^2 \sigma_0}{(4\pi)^3 H^4} \exp\left\{-\frac{4}{\gamma} \sin^2 E_R\right\} \exp\left\{-\frac{4c\tau}{\gamma H} \cos^2 E_R\right\}$,

$(1 + K^2)^2 = 1$ to a good approximation.

This integral can be evaluated simply by expressing each of the exponential terms as a power series and integrating the terms independently. Taking the Seasat 1 satellite's orbital and altimeter parameters to be the nominal one, the maximum value of $(4/\gamma)(c\tau/H)\sin^2 E_R$ is $\sim 2 \times 10^{-6}$ where $4/\gamma = 7.112 \times 10^3$, $E_{R_{max}} = \frac{1}{2}^o$, $c = 3 \times 10^8$, $\tau_{max} = 10^{-7}$ seconds and $H = 8 \times 10^5$. Consequently the contribution of $\exp((4/\gamma)(c\tau/H) \times \sin^2 E_R \cos\phi)$ will be virtually constant, *ie* independent of τ and have a value of unity to a very good order of approximation. Thus the integral reduces to:

$$P(\tau) = A \int_{\phi} \delta\left(\tau - \frac{2}{c}(R - H)\right) \exp\left\{\frac{4}{\gamma}\left(\frac{c\tau}{H}\right)^{\frac{1}{2}} \sin 2E_R \cos\phi\right\} \rho d\phi \quad .$$

Let $\alpha_1 = \frac{4}{\gamma}\left(\frac{c\tau}{H}\right)^{\frac{1}{2}} \sin 2E_R$, then:

$$\exp(\alpha_1 \cos\phi) = 1 + \alpha_1 \cos\phi + \frac{\alpha_1^2}{2!}\cos^2\phi + \frac{\alpha_1^3}{3!}\cos^3\phi + \ldots \quad .$$

As $\int_0^{2\pi} \cos^n\phi \, d\phi$ is zero if n is odd, and

$$\int_0^{2\pi} \cos^2\phi \, d\phi = \pi \, , \qquad \int_0^{2\pi} \cos^4\phi \, d\phi = \frac{3}{4}\pi \, , \qquad \int_0^{2\pi} \cos^6\phi \, d\phi = \frac{5}{8}\pi$$

and

$$\int_0^{2\pi} \cos^8\phi \, d\phi = \frac{35}{64}\pi \, ,$$

then

$$\int_0^{2\pi} \exp(\alpha_1 \cos\phi) d\phi = 2\pi + \frac{\alpha_1^2}{2!}\pi + \frac{\alpha_1^4}{4!}\frac{3}{4}\pi + \frac{\alpha_1^6}{6!}\frac{5}{8}\pi + \frac{\alpha_1^8}{8!}\frac{35}{64}\pi + \ldots \quad .$$

Consequently

$$P(\tau) = 2\pi A\left(1 + \alpha^2 + \frac{\alpha^4}{16} + \frac{\alpha^6}{576} + \ldots\right)$$

where $\alpha = \frac{4c\tau}{\gamma^2 H}\sin^2 2E_R$.

As the maximum value of $\alpha = 0.38$ for $|\tau| \leq 100$ ns and the preceding Seasat 1 values then $\alpha^2 = 0.1451$, $\alpha^4/16 = 0.0013$ and $\alpha^6/576 = 5 \times 10^{-6}$. Thus $\alpha^2 \gg \alpha^4 \gg \alpha^6$ so $P(\tau) = 2\pi A(1 + \alpha^2)$ to a good order of approximation.

So the evaluation of $P(\tau)$ gives:

$$\frac{2\pi\lambda^2 G_0^2 \sigma_0}{(4\pi)^3 H^4} \exp\left\{-\frac{4}{\gamma}\sin^2 E_R\right\} \exp\left\{-\frac{4c\tau}{\gamma H}\cos^2 E_R\right\}(1+\alpha^2) \quad .$$

This description is valid for $\tau \geq 0$. For $\tau < 0$, $P(t) = 0$.

Appendix B

EVALUATION OF THE CONVOLUTION OF THE WAVE JOINT HEIGHT AND SLOPE PROBABILITY DISTRIBUTION AND THE TRANSMITTED PULSE DISTRIBUTION

In the derivation of a received pulse's mean envelope two convolution integrals have to be evaluated (see section 3.5), this Appendix is concerned with the first of these. The two functions being convolved are the waveheight pdf (probability density function) and a function describing a transmitted pulse's shape.

From section 3.3 the waveheight pdf expressed in terms of time is:

$$\left(2\pi\sigma_w^2\right)^{-\frac{1}{2}} \exp\left(-\frac{(ct)^2}{8\sigma_w^2}\right)\left\{1 + \lambda_1\left(\frac{\left((ct)^3/8\sigma_w^2\right) - (9ct)/2\sigma_w}{6}\right)\right\}, \quad \text{as} \quad z = ct/2,$$

while the mean pulse shape is described by the function:

$$\left(2\pi\sigma_p^2\right)^{-\frac{1}{2}} \exp\left(-\frac{t^2}{2\sigma_p^2}\right) .$$

If A and B are two functions that are being convolved then from Fourier transform theory:

$$FT(A * B) = FT(A) \times FT(B)$$

and

$$A * B = FT^{-1}(FT(A) \times FT(B)) .$$

Here * denotes the convolution process, FT the operation of a Fourier transform, and FT^{-1} the operation of an inverse Fourier transform. From contour integration it is found that

$$FT(\exp(-\beta t^2)) = \left(\frac{\pi}{\beta}\right)^{\frac{1}{2}} \exp\left(-\frac{w^2}{4\beta}\right) ,$$

consequently

$$FT\left(\left(2\pi\sigma_p^2\right)^{-\frac{1}{2}} \exp\left(-\frac{t^2}{2\sigma_p^2}\right)\right) = \exp\left(-\frac{w^2\sigma_p^2}{2}\right) .$$

The second Fourier transform is:

$$FT\left\{\left(2\pi\sigma_w^2\right)^{-\frac{1}{2}} \exp\left(-\frac{(ct)^2}{8\sigma_w^2}\right)\left(1 + \lambda_1 \frac{\left((ct)^3/8\sigma_w^2\right) - (9ct/2\sigma_w)}{6}\right)\right\} .$$

In solving this last integral let $Q = c^2/8\sigma_w^2$. Rewriting this integral in its component parts one gets:

$$\left(2\pi\sigma_w^2\right)^{-\frac{1}{2}}\left\{\int_{-\infty}^{\infty} \exp(-Qt^2)\,\exp(j\omega t)dt + \frac{\lambda_1 c^3}{48\sigma_w^3}\int_{-\infty}^{\infty} t^3\exp(-Qt^2)\,\exp(j\omega t)dt - \frac{3\lambda_1 c}{4\sigma_w}\int_{-\infty}^{\infty} t\exp(-Qt^2)\,\exp(j\omega t)dt\right\} . \qquad (B\text{-}1)$$

As

$$\int_{-\infty}^{\infty} \exp(-Qt^2)\,\exp(j\omega t)dt = \left(\frac{\pi}{Q}\right)^{\frac{1}{2}}\exp\left(-\frac{w^2}{4Q}\right)$$

solutions to the integrals involving t^3 and t terms can be easily derived as follows: Letting

$$c \equiv \int_{-\infty}^{\infty} \exp(-Qt^2)\,\exp(j\omega t)dt$$

then:

$$\frac{d}{dw}c = jtc\,, \qquad \frac{d^2c}{dw^2} = -t^2c \qquad \text{and} \qquad \frac{d^3c}{dw^3} = -jt^3c\,.$$

As c is also equivalent to $(\pi/Q)^{\frac{1}{2}}\exp(-w^2/4Q)$ then:

$$jtc = -\left(\frac{w}{2Q}\right)\left(\frac{\pi}{Q}\right)^{\frac{1}{2}}\exp\left(-\frac{w^2}{4Q}\right),$$

$$-t^2c = \left(\frac{1}{2Q}\right)\left(\frac{\pi}{Q}\right)^{\frac{1}{2}}\left(\frac{w^2}{2Q}-1\right)\exp\left(-\frac{w^2}{4Q}\right)$$

and

$$-jt^3c = \left(\frac{1}{2Q}\right)\left(\frac{\pi}{Q}\right)^{\frac{1}{2}}\left(\frac{3w}{2Q}-\frac{w^3}{4Q^2}\right)\exp\left(-\frac{w^2}{4Q}\right).$$

Consequently the solution of integral (B-1) is:

$$\frac{2}{c}\exp\left(-\frac{w^2}{4Q}\right)\left[1 - \frac{j3\lambda_1 cw}{8\sigma_w Q} + j\left(\frac{1}{2Q}\right)\frac{\lambda_1 c^3}{48\sigma_w^3}\left(\frac{3w}{2Q}-\frac{w^3}{4Q^2}\right)\right].$$

Hence the product of the two Fourier transforms is:

$$\left(\frac{2}{c}\right)\exp\left(-\left(\frac{1}{4Q}+\frac{\sigma_p^2}{2}\right)w^2\right)\left[1 - \frac{j3\lambda_1 cw}{8\sigma_w Q} + j\left(\frac{1}{2Q}\right)\frac{\lambda_1 c^3}{48\sigma_2^3}\left(\frac{3w}{2Q}-\frac{w^3}{4Q^2}\right)\right].$$

Consequently the inverse Fourier transform is:

$$\frac{1}{2\pi}\int_{-\infty}^{\infty} U \exp(-Vw^2)(1 + jXw - jYw^3)\exp(-j\omega t)dw \qquad (B\text{-}2)$$

where $U = 2/c$, $V = (1/4Q) + (\sigma p^2/2)$, $X = 3\lambda_1 c/8\sigma_w Q\left(c^2/24\sigma_w^2 Q - 1\right)$ and $Y = \lambda_1 c^3/384Q^3\sigma_w^3$.

This integral is solved in the same manner as the previous one. Setting

$$C \equiv \int \exp(-Vw^2)\exp(-j\omega t)dt = \left(\frac{\pi}{V}\right)^{\frac{1}{2}} \exp\left(-\frac{t^2}{4V}\right)$$

then

$$\frac{dc}{dt} = -j\omega c = -\left(\frac{t}{2V}\right)\left(\frac{\pi}{V}\right)^{\frac{1}{2}} \exp\left(-\frac{t^2}{4V}\right),$$

$$\frac{d^2c}{dt^2} = -\omega^2 c = \left(\frac{1}{2V}\right)\left(\frac{\pi}{V}\right)^{\frac{1}{2}}\left(\frac{t^2}{2V} - 1\right)\exp\left(-\frac{t^2}{4V}\right)$$

and

$$\frac{d^3c}{dt^3} = +j\omega^3 c = \left(\frac{1}{2V}\right)\left(\frac{\pi}{V}\right)^{\frac{1}{2}}\left(\frac{3t}{2v} - \frac{t^3}{4V^2}\right)\exp\left(-\frac{t^2}{4V}\right).$$

Consequently the solution of (B-2) is

$$\frac{u}{2(V\pi)^{\frac{1}{2}}}\exp\left(-\frac{t^2}{4V}\right)\left[1 + \frac{Xt}{2V} + \left(\frac{Y}{2V}\right)\left(\frac{t^3}{4V^2} - \frac{3t}{2V}\right)\right].$$

Thus a function describing the result of the convolution of the wave pdf and pulse shape distributions has been produced. This result is used in Appendix C.

Appendix C

DEVELOPMENT OF THE QUANTITATIVE DESCRIPTION OF A MEAN WAVEFORM

As mentioned in section 3.5 the quantitative description of a waveform P_w results from the following convolution procedure:

$$P_w = I_p * W_h * P_D * I_T$$

where I_p is the impulse response, W_h the joint wave height/slope pdf, P_D the distribution describing the pulse shape, I_T the instrument transfer function, and * denotes a convolution process. The convolutions can take place in any order. The convolution of W_h with P_D is given in Appendix B; this Appendix is concerned with the remaining two convolutions, *ie* $I_p * T * I_T$ where $T = W_h * P_D$.

Evaluation of $T * I_T$

From Appendix B:

$$T = \frac{u}{2(V\pi)^{\frac{1}{2}}} \exp\left(-\frac{\tau^2}{4V}\right)\left(1 + \frac{X\tau}{2V} + \frac{Y}{2V}\left(\frac{\tau^3}{4V^2} - \frac{3\tau}{2V}\right)\right)$$

and

$$\left.\begin{aligned} I_T &= 1 \\ &= 0 \end{aligned}\right\} \qquad \begin{aligned} &\tau_1 < \tau < \tau_2 \\ &\tau < \tau_1, \quad \tau > \tau_2. \end{aligned}$$

Consequently the integral representation of the convolution is:

$$\int_{\tau_1}^{\tau_2} \left(1 + F(t-\tau) + G(t-\tau)^3\right) \exp\left(-e(t-\tau)^2\right) d\tau$$

where $F = (X/2V) - (3Y/4V^2)$, $G = Y/8V^3$ and $e = 1/4V$.

Substituting $T = e^{\frac{1}{2}}(t-\tau)$ then $-dT/e^{\frac{1}{2}} = d\tau$, $T_2 = e^{\frac{1}{2}}(t-\tau_2)$ and $T_1 = e^{\frac{1}{2}}(t-\tau_1)$.

So the integral can now be expressed as:

$$\frac{1}{e^{\frac{1}{2}}}\left\{\int_{T_2}^{T_1} \exp(-T^2)dT + \frac{F}{e^{\frac{1}{2}}}\int_{T_2}^{T_1} T\exp(-T^2)dT + \frac{G}{e^{\frac{3}{2}}}\int_{T_2}^{T_1} T^3\exp(-T^2)dT\right\} .$$

The solution of the first integral is in terms of the error function, *ie*

$$\frac{1}{e^{\frac{1}{2}}}\int_{T_2}^{T_1} \exp(-T^2)dT = 0.5\sqrt{\frac{\pi}{e}}\left(\mathrm{erf}(T_1) - \mathrm{erf}(T_2)\right) .$$

For the second integral

$$\frac{F}{e}\int_{T_2}^{T_1} T\exp(-T^2)dT = \frac{F}{2e}\left\{\exp\left(-T_2^2\right) - \exp\left(-T_1^2\right)\right\} .$$

To solve the third, consider

$$\frac{d}{dT}T^2\exp(-T^2) = -2T^3\exp(-T^2) + 2T\exp(-T^2)$$

then
$$\int_{T_2}^{T_1} T^3\exp(-T^2)dT = 2\int_{T_2}^{T_1} T\exp(-T^2)dT - T^2\exp(-T^2)\Big|_{T_2}^{T_1} ,$$

therefore
$$\frac{G}{e^2}\int_{T_2}^{T_1} T^3\exp(-T^2)dT = \frac{G}{e^2}\left\{\left(1+T_2^2\right)\exp\left(-T_2^2\right) - \left(1+T_1^2\right)\exp\left(-T_1^2\right)\right\} .$$

Consequently the solution of $T * I_T$ is:

$$0.5\sqrt{\frac{\pi}{e}}\left\{\operatorname{erf}(T_1) - \operatorname{erf}(T_2)\right\} + \left(\frac{F}{2e} + \frac{G}{e^2}\left(1+T_2^2\right)\right)\exp\left(-T_2^2\right)$$
$$- \left(\frac{F}{2e} + \frac{G}{e^2}\left(1+T_1^2\right)\right)\exp\left(-T_1^2\right) .$$

The desired quantitative waveform description can now be obtained by evaluating:

$$B\int_0^{\infty}(1+a_1t)\exp(-ft)\left\{\frac{1}{2}\sqrt{\frac{\pi}{e}}\left(\operatorname{erf}(T_1') - \operatorname{erf}(T_2')\right) + \left(\frac{F}{2e} + \frac{G}{e^2}\right)\left(\exp\left(-T_2'^2\right) - \exp\left(-T_1'^2\right)\right)\right\}$$
$$+ \frac{G}{e^2}\left\{T_2'^2\exp\left(-T_2'^2\right) - T_1'^2\exp\left(-T_1'^2\right)\right\}dt ,$$

where $B = \dfrac{2\pi\lambda^2G_0^2\sigma_0}{(4\pi)^3H^4}\dfrac{u}{2(\pi V)^{\frac{1}{2}}}\exp\left(-\dfrac{4}{\gamma}\sin^2E_R\right)$,

$$f = \frac{4c}{\gamma H}\cos^2E_R , \qquad a_1 = \frac{4c}{\gamma^2H}\sin^2 2E_R ,$$

$$T_1' = e^{\frac{1}{2}}(w_1 - t) \qquad (w_1 = s - \tau_1)$$

and
$$T_2' = e^{\frac{1}{2}}(w_2 - t) \qquad (w_2 = s - \tau_2) .$$

This integral splits into six parts:

$$\text{Part (1)} \qquad \frac{B}{2}\sqrt{\frac{\pi}{e}} \int_0^\infty \left(\operatorname{erf}(T_1') - \operatorname{erf}(T_2')\right) \exp(-ft)dt$$

$$\text{Part (2)} \qquad B\left(\frac{F}{2e} + \frac{G}{e^2}\right) \int_0^\infty \left(\exp\left(-T_2'^2\right) - \exp\left(-T_1'^2\right)\right) \exp(-ft)dt$$

$$\text{Part (3)} \qquad \frac{BG}{e^2} \int_0^\infty \left(T_2'^2 \exp\left(-T_2'^2\right) - T_1'^2 \exp\left(-T_1'^2\right)\right) \exp(-ft)dt$$

$$\text{Part (4)} \qquad \frac{B}{2}\sqrt{\frac{\pi}{e}}\, a_1 \int_0^\infty t\left(\operatorname{erf}(T_1') - \operatorname{erf}(T_2')\right) \exp(-ft)dt$$

$$\text{Part (5)} \qquad B\left(\frac{F}{2e} + \frac{G}{e^2}\right) a_1 \int_0^\infty t\left(\exp\left(-T_2'^2\right) - \exp\left(-T_1'^2\right)\right) \exp(-ft)dt$$

$$\text{Part (6)} \qquad \frac{BGa_1}{e^2} \int_0^\infty t\left(T_2'^2 \exp\left(-T_2'^2\right) - T_1'^2 \exp\left(-T_1'^2\right)\right) \exp(-ft)dt \ .$$

Evaluating part (1)

Integral is of the form

$$\int_0^\infty \operatorname{erf}(T) \exp(-ft)dt \ .$$

As $T = e^{\frac{1}{2}}(w - t)$ then $dt = -dT/e^{\frac{1}{2}}$, and

$$\int_0^\infty \operatorname{erf}(T) \exp(-ft)dt = -\frac{1}{e^{\frac{1}{2}}} \int_{e^{\frac{1}{2}}w}^{-\infty} \operatorname{erf}(T) \exp\left(-f\left(w - \frac{T}{e^{\frac{1}{2}}}\right)\right) dT \ .$$

Set $\gamma = fw$, $\eta = f/e^{\frac{1}{2}}$.

As

$$\frac{d}{dT} \operatorname{erf}(T) \exp(-(\gamma - \eta T)) = \operatorname{erf}(T)\eta \exp(-(\gamma - \eta T)) + \frac{2}{\sqrt{\pi}} \exp(-T^2) \exp(-(\gamma - \eta T))$$

then

$$\int_{e^{\frac{1}{2}}w}^{-\infty} \operatorname{erf}(T)\exp(-(\gamma - \eta T))dT = \frac{1}{\eta}\left\{-\frac{2}{\sqrt{\pi}}\int_{e^{\frac{1}{2}}w}^{-\infty}\exp(-T^2)\exp(-(\gamma-\eta T))dT + \operatorname{erf}(T)\exp(-(\gamma-\eta T))\Big|_{e^{\frac{1}{2}}w}^{-\infty}\right\} .$$

Evaluating $\int_{e^{\frac{1}{2}}w}^{-\infty} \exp(-T^2)\exp(-(\gamma-\eta T))dT$.

Completing the square this integral can be written as

$$\exp\left(\frac{\eta^2}{4}-\gamma\right)\int_{e^{\frac{1}{2}}w}^{-\infty}\exp\left(-\left(T-\frac{\eta}{2}\right)^2\right)dT = \exp\left(\frac{\eta^2}{4}-\gamma\right)\int_{e^{\frac{1}{2}}w-(\eta/2)}^{-\infty}\exp(-S^2)dS$$

$$= -\frac{\sqrt{\pi}}{2}\exp\left(\frac{\eta^2}{4}-\gamma\right)\left(1+\operatorname{erf}\left(e^{\frac{1}{2}}w-\frac{\eta}{2}\right)\right)$$

where $S = T - \frac{\eta}{2}$. Consequently

$$\int_0^{\infty}\operatorname{erf}(T)\exp(-ft)dt = \frac{1}{\eta e^{\frac{1}{2}}}\left[\operatorname{erf}(e^{\frac{1}{2}}w) - \exp\left(\frac{\eta^2}{4}-\gamma\right)\left(1+\operatorname{erf}\left(e^{\frac{1}{2}}w-\frac{\eta}{2}\right)\right)\right] .$$

Hence part (1) equals:

$$\frac{B\sqrt{\pi}}{2\eta e}\left\{\operatorname{erf}\left(e^{\frac{1}{2}}w_1\right) - \exp\left(\frac{f^2}{4e}-fw_1\right)\left(1+\operatorname{erf}\left(e^{\frac{1}{2}}w_1-\frac{f}{2e^{\frac{1}{2}}}\right)\right) - \operatorname{erf}\left(e^{\frac{1}{2}}w_2\right) + \exp\left(\frac{f^2}{4e}-fw_2\right)\left(1+\operatorname{erf}\left(e^{\frac{1}{2}}w_2-\frac{f}{2e^{\frac{1}{2}}}\right)\right)\right\} .$$

<u>Evaluating part (2)</u>

This integral is of the form

$$\int_0^{\infty}\exp(-T^2)\exp(-ft)dt .$$

As $T = e^{\frac{1}{2}}(w - t)$ by completing the square this integral becomes:

$$\exp\left(\frac{\eta^2}{4} - \gamma\right)\int_0^\infty \exp(-\, e(t + \alpha)^2)dt$$

where $\alpha = \frac{1}{2}\left(\frac{f}{e} - 2w\right)$.

Substituting $S = e^{\frac{1}{2}}(t + \alpha)$ one gets

$$\frac{1}{e^{\frac{1}{2}}} \exp\left(\frac{\eta^2}{4} - \gamma\right) \int_{e^{\frac{1}{2}}\alpha}^\infty \exp(-\, S^2)dS \;=\; \exp\left(\frac{\eta^2}{4} - \gamma\right)\frac{1}{2}\sqrt{\frac{\pi}{e}}\,(1 - \operatorname{erf}(e^{\frac{1}{2}}\alpha)) \quad .$$

Consequently part (2) equals:

$$B\left(\frac{F}{2e} + \frac{G}{e^2}\right)\frac{1}{2}\sqrt{\frac{\pi}{e}}\left\{\exp\left(\frac{f^2}{4e} - fw_2\right)\left(1 - \operatorname{erf}\left(\frac{f}{2e^{\frac{1}{2}}} - e^{\frac{1}{2}}w_2\right)\right)\right.$$
$$\left. - \exp\left(\frac{f^2}{4e} - fw_2\right)\left(1 - \operatorname{erf}\left(\frac{f}{2e^{\frac{1}{2}}} - e^{\frac{1}{2}}w_1\right)\right)\right\} \quad .$$

Evaluating part (3)

This part contains integrals of the form:

$$\int_0^\infty T^2 \exp(-\, T^2)\, \exp(-\, ft)dt \quad .$$

As $T = e^{\frac{1}{2}}(w - t)$ rewriting this integral one gets:

$$\frac{1}{e^{\frac{1}{2}}} \exp\left(\frac{f^2}{4e} - fw\right) \int_{-\infty}^{e^{\frac{1}{2}}w} T^2 \exp\left(-\left(T - \frac{f}{2e^{\frac{1}{2}}}\right)^2\right)dT \quad .$$

Let $\alpha = \frac{f}{2e^{\frac{1}{2}}}$. As

$$\frac{d}{dT}\, T \exp(-\,(T - \alpha)^2) \;=\; \exp(-\,(T - \alpha)^2) - 2T(T - \alpha)\exp(-\,(T - \alpha)^2)$$

then

$$\int_{-\infty}^{e^{\frac{1}{2}w}} T^2 \exp(-(T-\alpha)^2)dT = \frac{1}{2}\int_{-\infty}^{e^{\frac{1}{2}w}} \exp(-(T-\alpha)^2)dT - \tfrac{1}{2}T\exp(-(T-\alpha)^2)\Big|_{-\infty}^{e^{\frac{1}{2}w}} + \alpha\int_{-\infty}^{e^{\frac{1}{2}w}} T\exp(-(T-\alpha)^2)dT \quad .$$

From part (1)

$$\int_{-\infty}^{e^{\frac{1}{2}w}} \exp(-(T-\alpha)^2)dT = \tfrac{1}{2}\sqrt{\pi}\left(1 + \operatorname{erf}(e^{\frac{1}{2}w} - \alpha)\right) \quad .$$

Evaluating $\int_{-\infty}^{e^{\frac{1}{2}w}} T\exp(-(T-\alpha)^2)dT$. As

$$\frac{d}{dT}\exp(-(T-\alpha)^2) = -2(T-\alpha)\exp(-(T-\alpha)^2)$$

then

$$\int_{-\infty}^{e^{\frac{1}{2}w}} T\exp(-(T-\alpha)^2)dT = -\tfrac{1}{2}\exp(-(T-\alpha)^2)\Big|_{-\infty}^{e^{\frac{1}{2}w}} + \alpha\int_{-\infty}^{e^{\frac{1}{2}w}} \exp(-(T-\alpha)^2)dT$$

$$= -\tfrac{1}{2}\exp(-(e^{\frac{1}{2}w}-\alpha)^2) + \frac{\alpha\sqrt{\pi}}{2}\left(1 + \operatorname{erf}(e^{\frac{1}{2}w} - \alpha)\right) \quad ,$$

therefore

$$\int_0^{\infty} T^2\exp(-T^2)\exp(-ft)dt = \frac{1}{e^{\frac{1}{2}}}\exp\left(\frac{f^2}{4e} - fw\right)\left\{(\alpha^2 + \tfrac{1}{2})\frac{\sqrt{\pi}}{2}\left(1 + \operatorname{erf}(e^{\frac{1}{2}w} - \alpha)\right) - \tfrac{1}{2}(e^{\frac{1}{2}w} + \alpha)\exp(-(e^{\frac{1}{2}w} - \alpha)^2)\right\} \quad .$$

Thus part (3) equals:

$$\frac{GB}{e^{\frac{1}{2}}}\left[\exp\left(\frac{f^2}{4e}-fw_2\right)\left\{\left(\frac{f^2}{2e}+1\right)\frac{\sqrt{\pi}}{4}\left(1-\operatorname{erf}\left(\frac{f}{2e^{\frac{1}{2}}}-e^{\frac{1}{2}}w_2\right)\right)-\frac{1}{2}\left(\frac{f}{2e^{\frac{1}{2}}}+e^{\frac{1}{2}}w_2\right)\exp\left(-\left(\frac{f}{2e^{\frac{1}{2}}}-e^{\frac{1}{2}}w_2\right)^2\right)\right\}\right.$$

$$\left.-\exp\left(\frac{f^2}{4e}-fw_1\right)\left\{\left(\frac{f^2}{2e}+1\right)\frac{\sqrt{\pi}}{4}\left(1-\operatorname{erf}\left(\frac{f}{2e^{\frac{1}{2}}}-e^{\frac{1}{2}}w_1\right)\right)-\frac{1}{2}\left(\frac{f}{2e^{\frac{1}{2}}}+e^{\frac{1}{2}}w_1\right)\exp\left(-\left(\frac{f}{2e^{\frac{1}{2}}}-e^{\frac{1}{2}}w_1\right)^2\right)\right\}\right] .$$

Evaluation of part (4)

The integral here is of the form:

$$\int_0^\infty t\ \operatorname{erf}(T)\ \exp(-ft)dt \quad .$$

As $T = e^{\frac{1}{2}}(w - t)$ changing the variable of integration from t to T and substituting for the factor t one gets:

$$\underbrace{\frac{w}{e^{\frac{1}{2}}}\int_{-\infty}^{e^{\frac{1}{2}}w}\operatorname{erf}(T)\ \exp(-ft)dT}_{A}+\underbrace{\frac{1}{e}\int_{e^{\frac{1}{2}}w}^{-\infty}T\ \operatorname{erf}(T)\ \exp(-ft)dT}_{B} \quad .$$

The integral in component A has already been evaluated, as

$$\int_0^\infty \operatorname{erf}(T)\ \exp(-ft)dt = \frac{1}{e^{\frac{1}{2}}}\int_{-\infty}^{e^{\frac{1}{2}}w}\operatorname{erf}(T)\ \exp(-ft)dT$$

which from part (1) equals

$$\frac{1}{ne^{\frac{1}{2}}}\left[\operatorname{erf}(e^{\frac{1}{2}}w)-\exp\left(\frac{f^2}{4e}-fw\right)\left(1+\operatorname{erf}\left(e^{\frac{1}{2}}w-\frac{f}{2e^{\frac{1}{2}}}\right)\right)\right] ,$$

then denoting this by part (A) then component A equals $(w/ne^{\frac{1}{2}})$ · part (A).

Rewritting component B in the form

$$\frac{1}{e}\exp(-fw)\int_{e^{\frac{1}{2}}w}^{-\infty} T\,\mathrm{erf}(T)\,\exp\left(\frac{fT}{e^{\frac{1}{2}}}\right)dT$$

as

$$\frac{d}{dT}\left\{T\,\mathrm{erf}(T)\,\exp\left(\frac{fT}{e^{\frac{1}{2}}}\right)\right\} = \mathrm{erf}(T)\,\exp\left(\frac{fT}{e^{\frac{1}{2}}}\right) + \frac{2T}{\sqrt{\pi}}\exp(-T^2)\,\exp\left(\frac{fT}{e^{\frac{1}{2}}}\right) + \frac{f}{e^{\frac{1}{2}}}T\,\mathrm{erf}(T)\,\exp\left(\frac{fT}{e^{\frac{1}{2}}}\right)$$

then

$$\int_{e^{\frac{1}{2}}w}^{-\infty} T\,\mathrm{erf}(T)\,\exp\left(\frac{fT}{e^{\frac{1}{2}}}\right)dT = \frac{e^{\frac{1}{2}}}{f}\left[T\,\mathrm{erf}(T)\,\exp\left(\frac{fT}{e^{\frac{1}{2}}}\right)\Big|_{e^{\frac{1}{2}}w}^{-\infty} + \int_{-\infty}^{e^{\frac{1}{2}}w}\mathrm{erf}(T)\,\exp\left(\frac{fT}{e^{\frac{1}{2}}}\right)dT + \frac{2}{\sqrt{\pi}}\int_{-\infty}^{e^{\frac{1}{2}}w} T\exp(-T^2)\,\exp\left(\frac{fT}{e^{\frac{1}{2}}}\right)dT\right].$$

Evaluating the terms in the above expansion. From the above

$$\int_{-\infty}^{e^{\frac{1}{2}}w}\mathrm{erf}(T)\,\exp\left(\frac{fT}{e^{\frac{1}{2}}}\right)dT = \frac{1}{\eta}\exp(fw)\cdot \text{part (A)}\ .$$

As

$$\frac{2}{\sqrt{\pi}}\int_{-\infty}^{e^{\frac{1}{2}}w} T\exp(-T^2)\,\exp\left(\frac{fT}{e^{\frac{1}{2}}}\right)dT \quad \text{equals} \quad \frac{2}{\sqrt{\pi}}\exp\left(\frac{f^2}{4e}-fw\right)\int_{-\infty}^{e^{\frac{1}{2}}w} T\exp(-(T-\alpha)^2)dT$$

where $\alpha = f/2e^{\frac{1}{2}}$; and (from part (3)) as

$$\int_{-\infty}^{e^{\frac{1}{2}}w} T\exp(-(T-\alpha)^2)dT \quad \text{equals} \quad \frac{\alpha\sqrt{\pi}}{2}\left(1+\mathrm{erf}(e^{\frac{1}{2}}w-\alpha)\right) - \tfrac{1}{2}\exp(-(e^{\frac{1}{2}}w-\alpha))$$

then

$$\frac{2}{\sqrt{\pi}}\int_{-\infty}^{e^{\frac{1}{2}}w} T\exp(-T^2)\,\exp\left(\frac{fT}{e^{\frac{1}{2}}}\right)dT = \frac{1}{\sqrt{\pi}}\exp\left(\frac{f^2}{4e}-fw\right)\left[\alpha\sqrt{\pi}(1+\mathrm{erf}(e^{\frac{1}{2}}\alpha-w)) - \exp(-(e^{\frac{1}{2}}w-\alpha)^2)\right].$$

Consequently

$$\int_{e^{\frac{1}{2}}w}^{\infty} T\,\mathrm{erf}(T)\,\exp\left(\frac{fT}{e^{\frac{1}{2}}}\right)dT = \frac{e^{\frac{1}{2}}}{f}\left[-e^{\frac{1}{2}}w\,\mathrm{erf}(e^{\frac{1}{2}}w)\,\exp(fw) + \frac{1}{\eta}\exp(fw)\cdot\text{part (A)}\right.$$
$$\left. + \frac{1}{\sqrt{\pi}}\exp\left(\frac{f^2}{4e} - fw\right)\left(\alpha\sqrt{\pi}(1 + \mathrm{erf}(e^{\frac{1}{2}}w - \alpha)) - \exp(-(e^{\frac{1}{2}}w - \alpha)^2)\right)\right] ,$$

and therefore

$$\frac{1}{e}\int_{e^{\frac{1}{2}}w}^{\infty} T\,\mathrm{erf}(T)\,\exp(-ft)dT = \frac{1}{fe^{\frac{1}{2}}}\left[\frac{1}{\eta}\cdot\text{part (A)} - we^{\frac{1}{2}}\,\mathrm{erf}(e^{\frac{1}{2}}w)\right.$$
$$\left. + \frac{1}{\sqrt{\pi e}}\exp\left(\frac{f^2}{4e} - 2fw\right)\left\{\alpha\sqrt{\pi}(1 + \mathrm{erf}(e^{\frac{1}{2}}w - \alpha)) - \exp(-(e^{\frac{1}{2}}w - \alpha)^2)\right\}\right] .$$

The solution of part (4) is therefore:

$$\frac{B}{2}\sqrt{\frac{\pi}{e}}\,a_1\left[\frac{1}{\eta e^{\frac{1}{2}}}\left(w_1 + \frac{1}{f}\right)\cdot\text{part }(A_1) - \frac{w_1}{f}\,\mathrm{erf}\left(e^{\frac{1}{2}}w_1\right)\right.$$
$$\left. + \frac{1}{f\pi^{\frac{1}{2}}e^{\frac{3}{2}}}\exp\left(\frac{f^2}{4e} - 2fw_1\right)\left(\alpha\pi^{\frac{1}{2}}\left(1 + \mathrm{erf}\left(e^{\frac{1}{2}}w_1 - \alpha\right)\right) - \exp\left(-\left(e^{\frac{1}{2}}w_1 - \alpha\right)^2\right)\right)\right]$$

$$-\frac{B}{2}\sqrt{\frac{\pi}{e}}\,a_1\left[\frac{1}{\eta e^{\frac{1}{2}}}\left(w_2 + \frac{1}{f}\right)\cdot\text{part }(A_2) - \frac{w_2}{f}\,\mathrm{erf}\left(e^{\frac{1}{2}}w_2\right)\right.$$
$$\left. + \frac{1}{f\pi^{\frac{1}{2}}e^{\frac{3}{2}}}\exp\left(\frac{f^2}{4e} - 2fw_2\right)\left(\alpha\pi^{\frac{1}{2}}\left(1 + \mathrm{erf}\left(e^{\frac{1}{2}}w_2 - \alpha\right)\right) - \exp\left(-\left(e^{\frac{1}{2}}w_2 - \alpha\right)^2\right)\right)\right] ,$$

where $\text{part }(A_1) = \mathrm{erf}\left(e^{\frac{1}{2}}w_1\right) - \exp\left(\frac{f^2}{4e} - fw_1\right)\left(1 + \mathrm{erf}\left(e^{\frac{1}{2}}w_1 - \frac{f}{2e^{\frac{1}{2}}}\right)\right)$,

$$\text{part }(A_2) = \mathrm{erf}\left(e^{\frac{1}{2}}w_2\right) - \exp\left(\frac{f^2}{4e} - fw_2\right)\left(1 + \mathrm{erf}\left(e^{\frac{1}{2}}w_2 - \frac{f}{2e^{\frac{1}{2}}}\right)\right)$$

and

$$\alpha = \frac{f}{2e^{\frac{1}{2}}} , \quad \eta = \frac{f}{e^{\frac{1}{2}}} .$$

Evaluating part (5)

The integral of interest is of the form:

$$\int_0^\infty t \exp(-T^2) \exp(-ft)dt \quad .$$

As $T = e^{\frac{1}{2}}(w - t)$ this can be written as:

$$w\int_0^\infty \exp(-T^2) \exp(-ft)dt - \underbrace{\frac{1}{e^{\frac{1}{2}}} \int_0^\infty T \exp(-T^2) \exp(-ft)dt}_{B} \quad .$$

Utilizing the solution given in part (1) then

$$w\int_0^\infty \exp(-T^2) \exp(-ft)dt = w \exp\left(\frac{f^2}{4e} - fw\right) \frac{1}{2}\sqrt{\frac{\pi}{e}} \left(1 - \operatorname{erf}\left(\frac{f}{2e^{\frac{1}{2}}} - e^{\frac{1}{2}}w\right)\right) \quad .$$

To evaluate B, complete the square and change from t to T. On doing this B becomes

$$\frac{1}{e} \exp\left(\frac{f^2}{4e} - fw\right) \int_{e^{\frac{1}{2}}w}^{-\infty} T \exp(-(T - \alpha)^2)dT$$

where $\alpha = f/2e^{\frac{1}{2}}$. From part (3)

$$\int_{e^{\frac{1}{2}}w}^{-\infty} T \exp(-(T - \alpha)^2)dT = \tfrac{1}{2} \exp(-(e^{\frac{1}{2}}w - \alpha)^2) - \frac{\alpha\sqrt{\pi}}{2} (1 + \operatorname{erf}(e^{\frac{1}{2}}w - \alpha)) \quad ,$$

therefore

$$-\frac{1}{e^{\frac{1}{2}}} \int_0^\infty T \exp(-T^2) \exp(-ft)dt = \frac{1}{2e} \exp\left(\frac{f^2}{4e} - fw\right) \left[\exp(-(e^{\frac{1}{2}}w - \alpha)^2) - \frac{\alpha\sqrt{\pi}}{2} (1 + \operatorname{erf}(e^{\frac{1}{2}}w - \alpha))\right] \quad .$$

Consequently the solution of part (5) is:

$$B\left(\frac{F}{2e} + \frac{G}{e^2}\right)a_1\left[w_2 \exp\left(\frac{f^2}{4e} - fw_2\right) \times 0.5\sqrt{\frac{\pi}{e}}\left(1 - \operatorname{erf}\left(\alpha - e^{\frac{1}{2}}w_2\right)\right)\right.$$

$$\left. + \frac{1}{2e}\exp\left(\frac{f^2}{4e} - fw_2\right)\left\{\exp\left(-\left(e^{\frac{1}{2}}w_2 - \alpha\right)^2\right) - \alpha\sqrt{\pi}\left(1 + \operatorname{erf}\left(e^{\frac{1}{2}}w_2 - \alpha\right)\right)\right\}\right]$$

$$- B\,\frac{F}{2e} + \frac{G}{e^2}\,a_1\left[w_1 \exp\left(\frac{f^2}{4e} - fw_1\right) \times 0.5\sqrt{\frac{\pi}{e}}\left(1 - \operatorname{erf}\left(\alpha - e^{\frac{1}{2}}w_1\right)\right)\right.$$

$$\left. + \frac{1}{2e}\exp\left(\frac{f^2}{4e} - fw_1\right)\left\{\exp\left(-\left(e^{\frac{1}{2}}w_1 - \alpha\right)^2\right) - \alpha\sqrt{\pi}\left(1 + \operatorname{erf}\left(e^{\frac{1}{2}}w_1 - \alpha\right)\right)\right\}\right] \quad ,$$

where $\alpha = f/2e^{\frac{1}{2}}$.

Evaluating part (6)

The integral of interest is

$$\int_0^\infty tT^2 \exp(-T^2)\exp(-ft)dt \quad .$$

As $T = e^{\frac{1}{2}}(w - t)$ this can be written as:

$$w\int_0^\infty T^2 \exp(-T^2)\exp(-ft)dt - \underbrace{\frac{1}{e^{\frac{1}{2}}}\int_0^\infty T^3 \exp(-T^2)\exp(-ft)dt}_{B} \quad .$$

From part (3)

$$w\int_0^\infty T^2 \exp(-T^2)\exp(-ft)dt = \frac{w}{e^{\frac{1}{2}}}\exp\left(\frac{f^2}{4e} - fw\right)\left\{\left(\alpha^2 + \frac{1}{2}\right)\frac{\sqrt{\pi}}{2}\left(1 + \operatorname{erf}(e^{\frac{1}{2}}w - \alpha)\right)\right.$$

$$\left. - \tfrac{1}{2}(e^{\frac{1}{2}}w + \alpha)\exp\left(-(e^{\frac{1}{2}}w - \alpha)^2\right)\right\}$$

$$= w \cdot Q \quad .$$

Rewritting part B as

$$\frac{1}{e}\exp\left(\frac{f^2}{4e} - fw\right)\int_{e^{\frac{1}{2}}w}^{-\infty} T^3 \exp(-(T-\alpha)^2)dT$$

where $\alpha = f/2e^{\frac{1}{2}}$ and considering $d/dT\ (T^2 \exp(-(T-\alpha)^2)$ which equals $2T\exp(-(T-\alpha)^2) - 2T^2(T-\alpha)\exp(-(T-\alpha)^2)$ then

$$\int_{e^{\frac{1}{2}}w}^{-\infty} T^3 \exp(-(T-\alpha)^2)dT = \int_{e^{\frac{1}{2}}w}^{-\infty} T\exp(-(T-\alpha)^2)dT + \alpha\int_{e^{\frac{1}{2}}w}^{-\infty} T^2\exp(-(T-\alpha)^2)dT - \tfrac{1}{2}T^2\exp(-(T-\alpha)^2)\Big|_{e^{\frac{1}{2}}w}^{-\infty}.$$

From part (3):

$$\int_{e^{\frac{1}{2}}w}^{-\infty} T\exp(-(T-\alpha)^2)dT = \tfrac{1}{2}\exp(-(e^{\frac{1}{2}}w-\alpha)^2) - \frac{\alpha\sqrt{\pi}}{2}(1+\operatorname{erf}(e^{\frac{1}{2}}w-\alpha)).$$

From the above

$$\int_{e^{\frac{1}{2}}w}^{-\infty} T^2\exp(-(T-\alpha)^2)dT = -e^{\frac{1}{2}}\exp\left(-\left(\frac{f^2}{4e} - fw\right)\right)\cdot Q,$$

therefore

$$-\frac{1}{e^{\frac{1}{2}}}\int_0^{\infty} T^3\exp(-T^2)\exp(-ft)dt = \frac{1}{e}\exp\left(\frac{f^2}{4e} - fw\right)\times$$

$$\times\left[\tfrac{1}{2}\exp(-(e^{\frac{1}{2}}w-\alpha)^2) - \frac{\alpha\sqrt{\pi}}{2}(1+\operatorname{erf}(e^{\frac{1}{2}}w-\alpha))\right.$$

$$\left. - \alpha e^{\frac{1}{2}}\exp\left(-\left(\frac{f^2}{4e} - fw\right)\right)\cdot Q + \frac{ew^2}{2}\exp(-(e^{\frac{1}{2}}w-\alpha)^2)\right].$$

Consequently the solution to part (6) is:

$$\frac{BGa_1}{e^2}\left[w_2Q_2 + \frac{1}{e}\exp\left(\frac{f^2}{4e} - fw_2\right) \times \left\{0.5\exp\left(-\left(e^{\frac{1}{2}}w_2 - \alpha\right)^2\right) - \frac{\alpha\sqrt{\pi}}{2}\left(1 + \operatorname{erf}\left(e^{\frac{1}{2}}w_2 - \alpha\right)\right)\right.\right.$$
$$\left.\left. - \alpha e^{\frac{1}{2}}\exp\left(-\left(\frac{f^2}{4e} - fw_2\right)\right) \cdot Q + \frac{ew_2^2}{2}\exp\left(-\left(e^{\frac{1}{2}}w_2 - \alpha\right)^2\right)\right\}\right]$$

$$-\frac{BGa_1}{e^2}\left[w_1Q_1 + \frac{1}{e}\exp\left(\frac{f^2}{4e} - fw_1\right) \times \left\{0.5\exp\left(-\left(e^{\frac{1}{2}}w_1 - \alpha\right)^2\right) - \frac{\alpha\sqrt{\pi}}{2}\left(1 + \operatorname{erf}\left(e^{\frac{1}{2}}w_1 - \alpha\right)\right)\right.\right.$$
$$\left.\left. - \alpha e^{\frac{1}{2}}\exp\left(-\left(\frac{f^2}{4e} - fw_1\right)\right) \cdot Q + \frac{ew_1^2}{2}\exp\left(-\left(e^{\frac{1}{2}}w_1 - \alpha\right)^2\right)\right\}\right]$$

where $$Q_1 = \frac{1}{e^{\frac{1}{2}}}\exp\left(\frac{f^2}{4e} - fw_1\right)\left\{\left(\alpha^2 + \frac{1}{2}\right)\frac{\sqrt{\pi}}{2}\left(1 + \operatorname{erf}\left(e^{\frac{1}{2}}w_1 - \alpha\right)\right)\right.$$
$$\left. - \frac{1}{2}\left(e^{\frac{1}{2}}w_1 + \alpha\right)\exp\left(-\left(e^{\frac{1}{2}}w_1 - \alpha\right)^2\right)\right\},$$

$$Q_2 = \frac{1}{e^{\frac{1}{2}}}\exp\left(\frac{f^2}{4e} - fw_2\right)\left\{\left(\alpha^2 + \frac{1}{2}\right)\frac{\sqrt{\pi}}{2}\left(1 + \operatorname{erf}\left(e^{\frac{1}{2}}w_2 - \alpha\right)\right)\right.$$
$$\left. - \frac{1}{2}\left(e^{\frac{1}{2}}w_2 + \alpha\right)\exp\left(-\left(e^{\frac{1}{2}}w_2 - \alpha\right)^2\right)\right\}$$

and

$$\alpha = \frac{f}{2e^{\frac{1}{2}}}.$$

Appendix D

THE DISCRIMINATOR CURVE

A quantitative description of this curve is required, as mentioned in section 4.2, so that the tracking bias, *ie* the value of τ when $I(\tau) = 0$, can be calculated. This bias is used to correct the processed height values. The discriminator curve $I(\tau)$ is described by the expression $I(\tau) = M(\tau) - \alpha L(W + \tau)$ where M and L are the middle and late gates employed by the tracking gate, τ is the time offset, *ie* the displacement of the centre of the middle gate from the origin of the waveform's time axis while W is the width of both gates.

Appendix C gives the quantitative description of the output as received from the DFB. This output equals the convolution of the instrument transfer function with the waveform. As the instrument transfer function I_t has a 'top hat' form, *ie*

$$I_t = \left.\begin{matrix} 1 \\ 0 \end{matrix}\right\} \quad \begin{matrix} -\tau_1 \leq \tau \leq \tau_2 \\ \tau < -\tau_1, \quad \tau > \tau_2 \end{matrix}$$

and the middle and late gates are also 'top hat' functions, thus $M(\tau)$ is given by the solution in Appendix C where $\tau_1 = \tau_2 = W/2$ and likewise $L(W + \tau)$ is given by the same solution where $\tau_1 = W/2$ and $\tau_2 = 3W/2$. By using the above expression for $I(\tau)$, with $\alpha = 0.5$ the discriminator curve can be determined given W.

For a specified pulse width and value of α the tracking bias is dependent on σ_w (rms waveheight), λ (skewness), E_r (attitude error angle) and W. Knowing σ_w, λ and E_r, W is selected on the basis of minimising this bias - the gate widths used as a function of σ_w are given in Table 2. This condition ensures that the tracking gates always sample a linear portion of a discriminator curve ensuring high sensitivity and stability of the ATU. As an adaptive tracking gate system was used in the Seasat 1 altimeter the three gates comprising a tracking gate are of equal width W and are contiguous. By employing contiguous gates the bias variation with E_r is minimised.

Lastly as AGC employed in the altimeter system kept the integrated DFB output of 50 consecutive waveforms constant, for each position of the tracking gate during the convolution procedure the area of the waveform sampled by the DFB must be fixed at a constant level. This area determination and consequent adjustment were carried out numerically in the simulation process described in section 4.3.

Table 1

SEASAT 1 ALTIMETER PARAMETERS

Frequency	13.5 GHz	Pulse repetition frequency	1024 Hz
Bandwidth	320 MHz	System noise temperature	3364 K
Chirp pulse width	3.2 μs	Gain control	Automatic
Compressed pulse width	3.125 ns	Antenna main lobe gain	40 dB
Pulse compression ratio	1024	Antenna polarization	Linear
Peak transmitted power	2 kW	Antenna diameter	1 m

Table 2

GATE WIDTHS EMPLOYED IN CALCULATING THE TRACKING BIAS

Rms waveheight (m)	Gate width (ns)
5	68.75
4	59.375
3	43.75
2	34.375
1	18.75
0.5	12.50

Table 3

σ_w (m)	a (cm)	b (cm)	c (cm)	d (cm)	e (cm)	Offset (cm)	Error (cm)	SD 1 (cm)	SD 2 (cm)
5	12.5	12.6	18.4	23.1	20.2	17.4	8.7	19.5	4.7
4	11.9	12.2	16.2	16.9	15.1	14.5	7.5	16.3	2.3
3	10.7	10.8	15.3	13.4	11.9	12.4	6.6	14.1	2.0
2	10.3	10.3	10.2	13.4	8.4	10.5	5.0	11.6	1.8
1	9.4	9.1	9.1	11.6	7.2	9.3	3.4	9.9	1.6
0.5	8.7	8.0	8.7	11.1	6.1	8.5	2.1	8.7	1.8

σ_w - rms waveheight

a - prediction of results for SNR = 10 from SNR = 30, $\lambda = 0.2$

b - prediction of results for SNR = 10 from SNR = 20, $\lambda = 0.2$

c - results of SNR = 10, $\lambda = 0.2$

d - results of SNR = 10, $\lambda = 0.4$

e - results of SNR = 10, $\lambda = 0$

SD 1 - standard deviation of total correction

SD 2 - standard deviation in SD 1

LIST OF SYMBOLS AND ABBREVIATIONS

AGC	automatic gain control
ATU	adaptive tracking unit
c	speed of light
CW	continuous wave
D	displacement current
dA	element of area
DDG	digital delay generator
DDL	digital delay line
DFB	digital filter bank
e	eccentricity
EM	electromagnetic
E_r	attitude error angle
E_s	scattered far field electric vector
E_{js}	contribution by the jth element to $\underline{E}_s$
$\hat{\underline{e}}$	unit vector of the incident electric field
$\hat{\underline{e}}_z$	z component of $\hat{\underline{e}}$
FM	frequency modulated
FT	operation of the Fourier transform
FT^{-1}	operation of the inverse Fourier transform
G	power gain of the altimeter antenna
GHz	gigahertz
H	satellite altitude
$\underline{H}$	magnetic field vector
$\underline{H}_i$	magnetic field vector of the incident EM wave
$\underline{H}_s$	magnetic field vector of the scattered EM wave
h(x,y)	surface elevation at point x, y
HSWS	high speed wave sampler
$\underline{I}$	unit dyad
$I(\tau)$	tracking law output
$I_r(\tau)$	flat sea impulse response
$I_t(\tau)$	instrument transfer function
$\underline{J}$	current density
k	magnitude of the wave number vector
$\underline{k}_i$	wave number vector of the incident EM wave
$\underline{k}_s$	wave number vector of the scattered EM wave
K_j	Gaussian curvature at point j
kHz	kilohertz
L	power output of the late tracking gate
LO	local oscillator
LSB	least significant bit
M	power output of the middle tracking gate
MHz	megahertz

LIST OF SYMBOLS AND ABBREVIATIONS (concluded)

MSB	most significant bit
N	average number of specular points per unit area
$\hat{\underline{n}}$	unit vector normal to surface
$\hat{\underline{n}}_j$	unit vector normal to surface at the jth element
N_p	number of pulses averaged
ns	nanosecond
P	power output of altimeter transmitter
P(t)	power received from altimeter footprint at time t
pdf	probability density function
$p(\Delta x,\Delta y)$	slope pdf
$p(z;\Delta x,\Delta y)$	joint slope height pdf
$P_s(\tau)$	pulse shape distribution
R	radial distance between area element and altimeter
r	distance measurement in plane of the sea surface
R_i	principal radius of curvature at point i
rms	root mean square
SACU	synchroniser, acquisition and control unit
SNR	signal to noise ratio
t	time measurement with origin at time of pulse transmission
T_e	width of middle tracking gate
T_i	width of late tracking gate
T_p	point on leading edge tracked to
W	tracking gate width
$W(\tau)$	waveheight pdf
α_i	number of DFB gates comprising middle and late tracking gates
Δ	increment in a variable
$\Delta t'$	height resolution size
$\delta(\ )$	Dirac delta function
η	angle of incidence at each point j
θ	antenna beamwidth
λ	skewness coefficients
λ_i	wavelength of impinging radiation
μ	permeability constant
μs	microsecond
μ_{mn}	moment of the distribution $P(z;\Delta x)$
σ	backscatter cross section for a unit area of scattering surface
σ_R	rms tracking error
σ_P	rms width of the distribution describing the transmitted pulse shape
σ_w	rms waveheight
σ_z	standard deviation of surface elevations
$\sigma_{\Delta x}$	standard deviation of surface slopes in the x direction
τ	time measurement with origin at time of reception of signal from mean sea level
ω	angular frequency

REFERENCES

No.	Author	Title, etc
1	P. Ronal	Seasat - Interim Geophysical Data Record (IGDR) Users' Handbook - altimeter. Jet Propulsion Laboratory, 15 April 1979
2	L.S. Miller G.S. Brown	Engineering studies related to the GOES-C radar altimeter. NASA Report CR-137462 (1974)
3	J.L. MacArthur	Design of the Seasat-A radar altimeter. MTS-IEEE, Oceans '76, 10B1-10B8 (1976)
4	R.K. Moore C.S. Williams	Radar terrain at near vertical incidence. Proc. IRE, 45, 228-238 (1957)
5	J.K. Schindler	Electromagnetic scattering phenomena associated with extended surfaces. IEEE International Conv. Rec., 15 part 2, 136-149 (1967)
6	D.E. Barrick W.H. Peake	Review of scattering from surfaces with different roughness scales. Radio Science, 3, 865-868 (1968)
7	R.D. Kodis	A note on the theory of scattering from an irregular surface. IEEE Trans. Antennas Propagat, 14, 77-82 (1966)
8	V. Stein	Microwave scattering from the sea surface. RAE Library Translation 1956 (1978)
9	M.L. Burrows	A reformulated boundary perturbation theory in electromagnetism and its application to a sphere. Can. J. Phys., 45, 1729-1743 (1967)
10	G.S. Brown	Backscattering from a Gaussian-distributed perfectly conducting rough surface. IEEE Trans. Antennas Propagat., 26, 472-481 (1978)
11	M. Born E. Wolf	Principles of Optics 2nd rev. New York: Pergamon, 754 (1964)
12	D.E. Barrick	Rough surface scattering based on the specular point theory. IEEE Trans. Antennas Propagat., 16, 449-454 (1968)
13	B. Kinsman	Wind waves: their generation and propagation on the ocean surface. Prentice-Hall, Englewood Cliffs, New Jersey (1965)
14	M.S. Longuet-Higgins	The effect of non-linearities on statistical distributions in the theory of sea waves. J. Fluid Mech., 17, 459-481 (1963)

REFERENCES (concluded)

No.	Author	Title, etc
15	F.C. Jackson	The reflection of impulses from a nonlinear random sea. J. Geophys. Res., 84, 4939-4943 (1979)
16	G.S. Brown	The average impulse response of a rough sea and its applications. IEEE Trans. Antenna Propagat., 25, 67-74 (1977)
17	G.S. Hayne	Radar altimeter mean return wave forms from near normal incidence ocean surface scattering. Final Report, NASA Report CR-156864 (1980)
18	L.W. Brooks R.P. Dooley	Technical guidance and analytical services in support of Seasat-A. Final Report, NASA Report CR-141399 (1975)

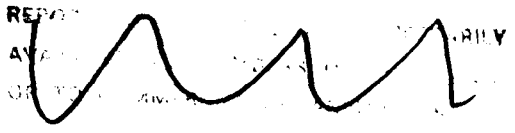

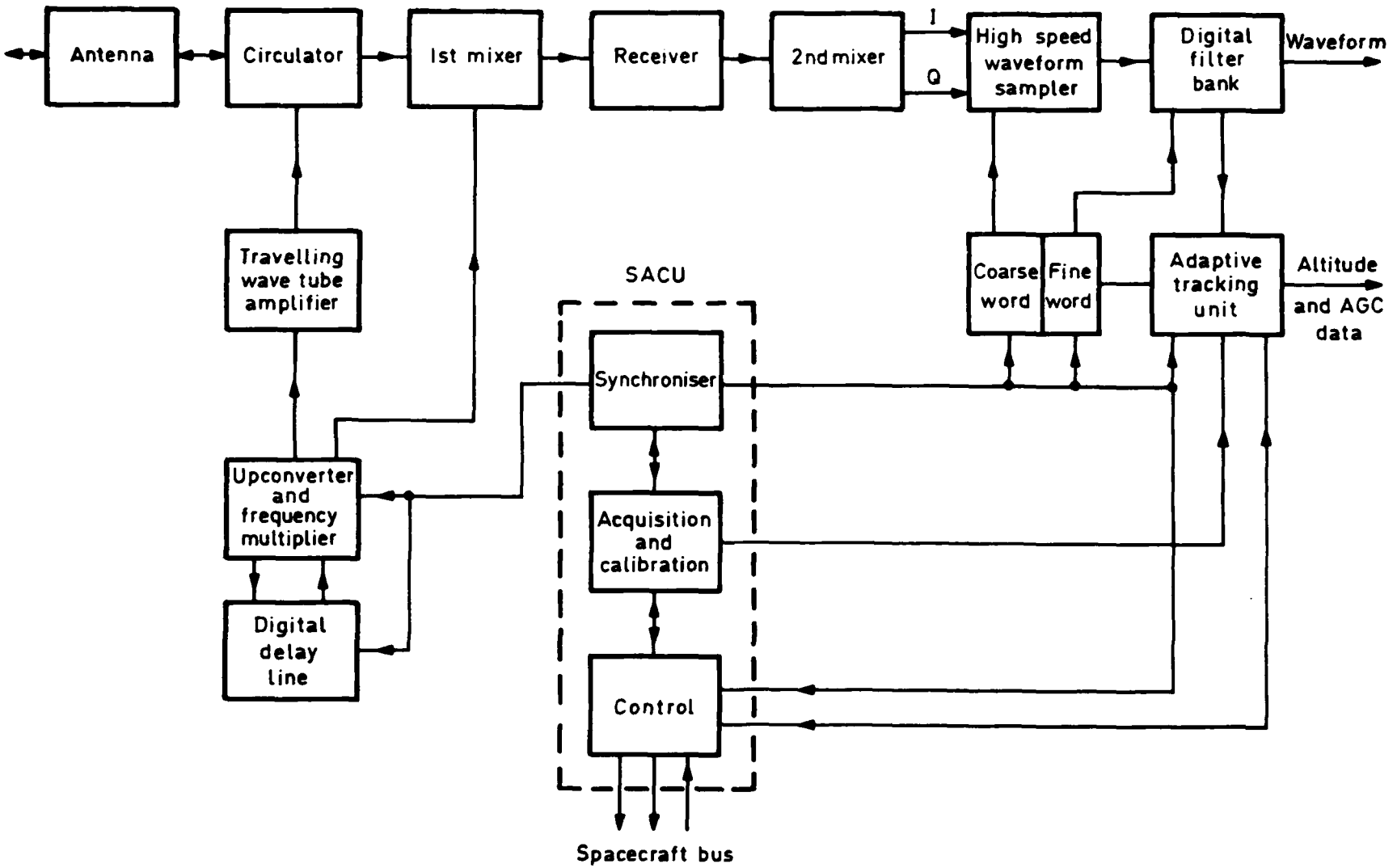

Fig 1 Schematic of the Seasat 1 altimeter system

Fig 1

Fig 2

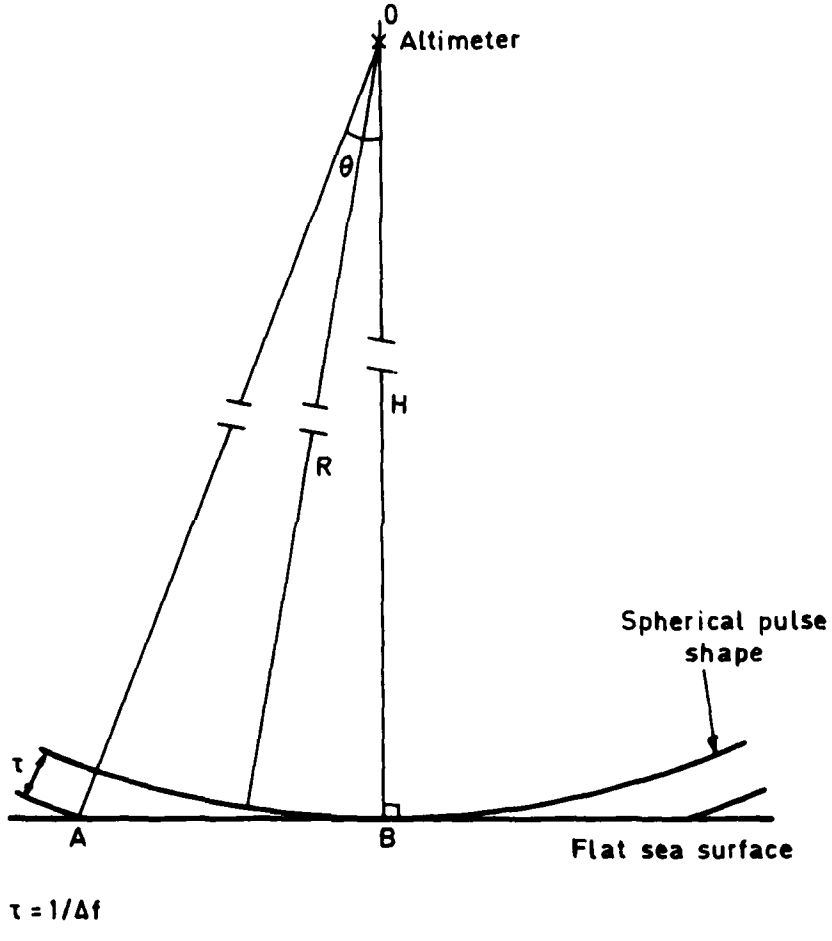

$\tau = 1/\Delta f$

Fig 2 Geometry illustrating the interaction of a spherical pulse with a flat sea surface

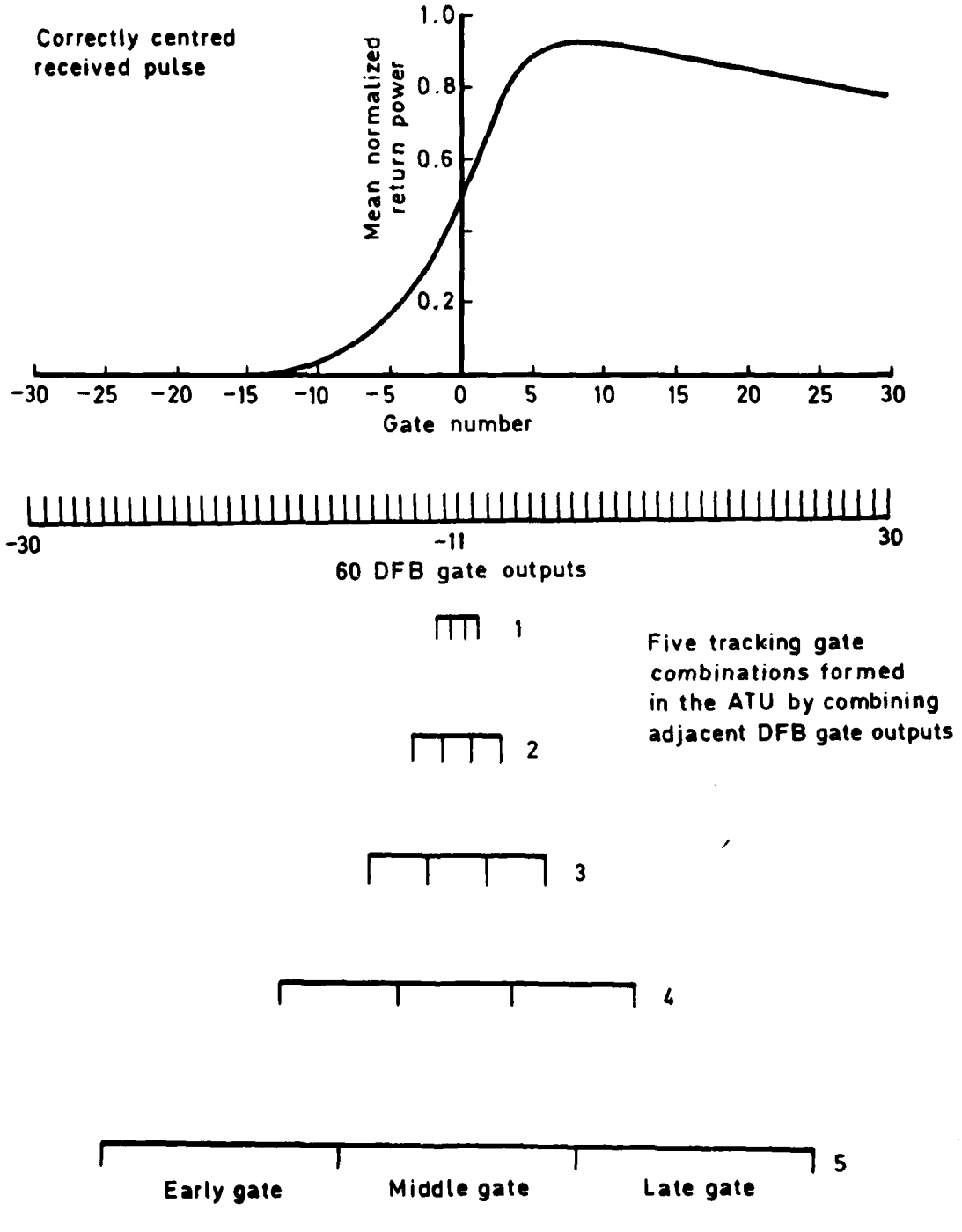

Fig 3 **Formation of the five tracking gate combinations and their positioning with respect to a correctly centred pulse**

Fig 4

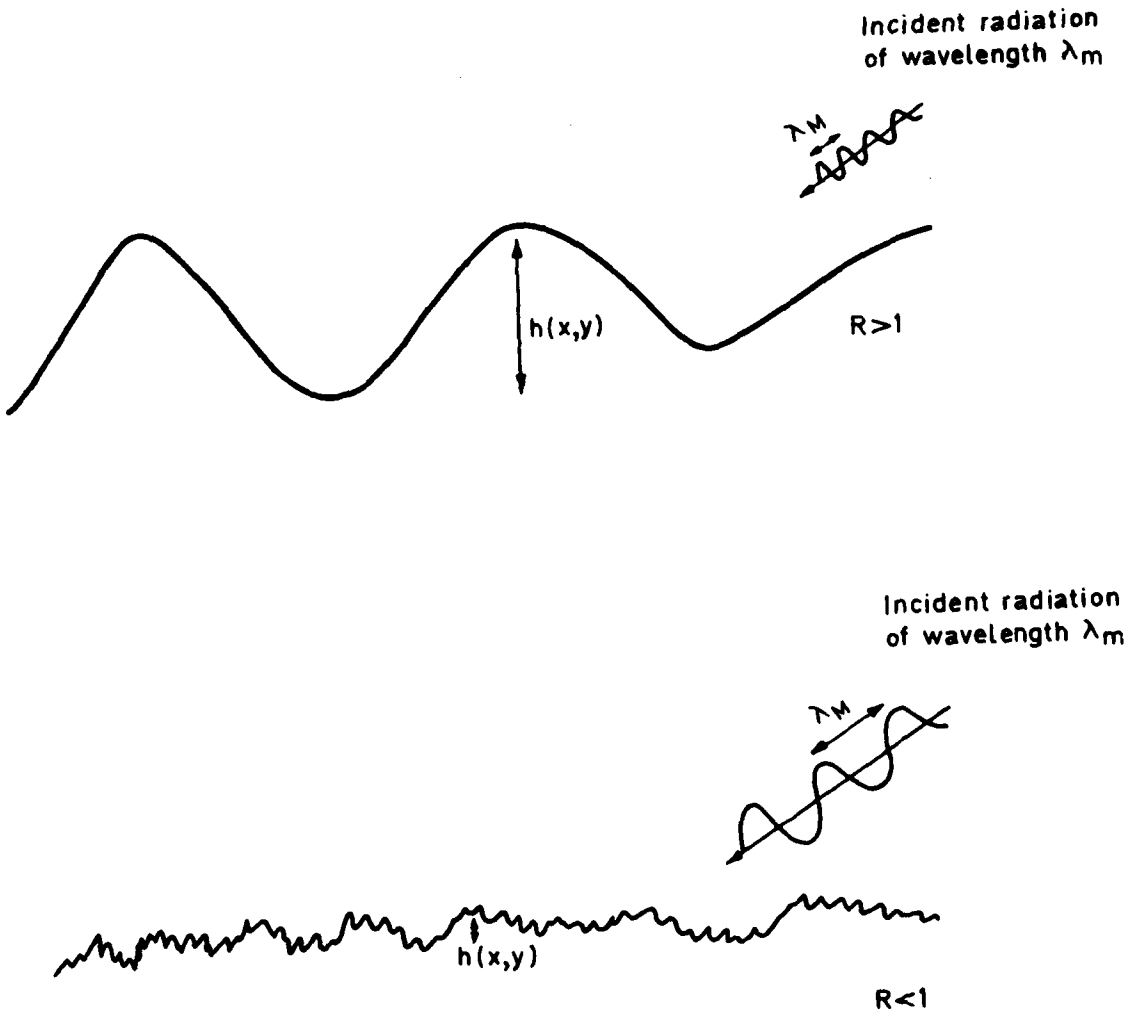

Fig 4 Illustration of two typical scattering surfaces.
Top — smoothly varying surface where $R > 1$
Bottom — rough surface where $R < 1$
(h(x,y) — surface elevation at point x,y)

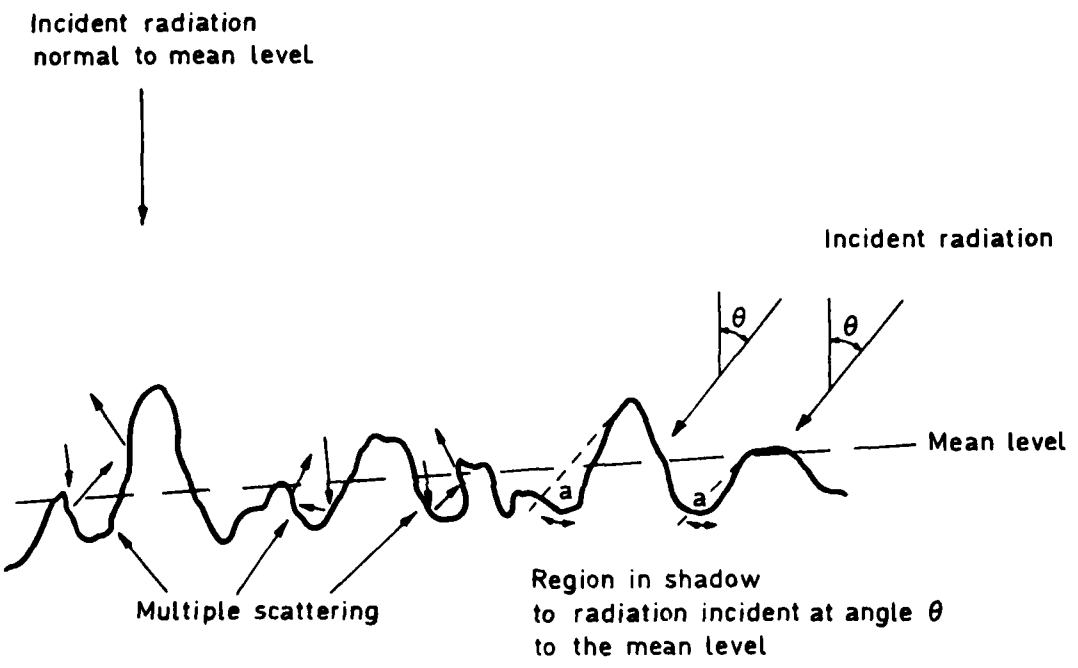

Fig 5 Surface exhibiting multiple scattering and shadowing

Fig 6

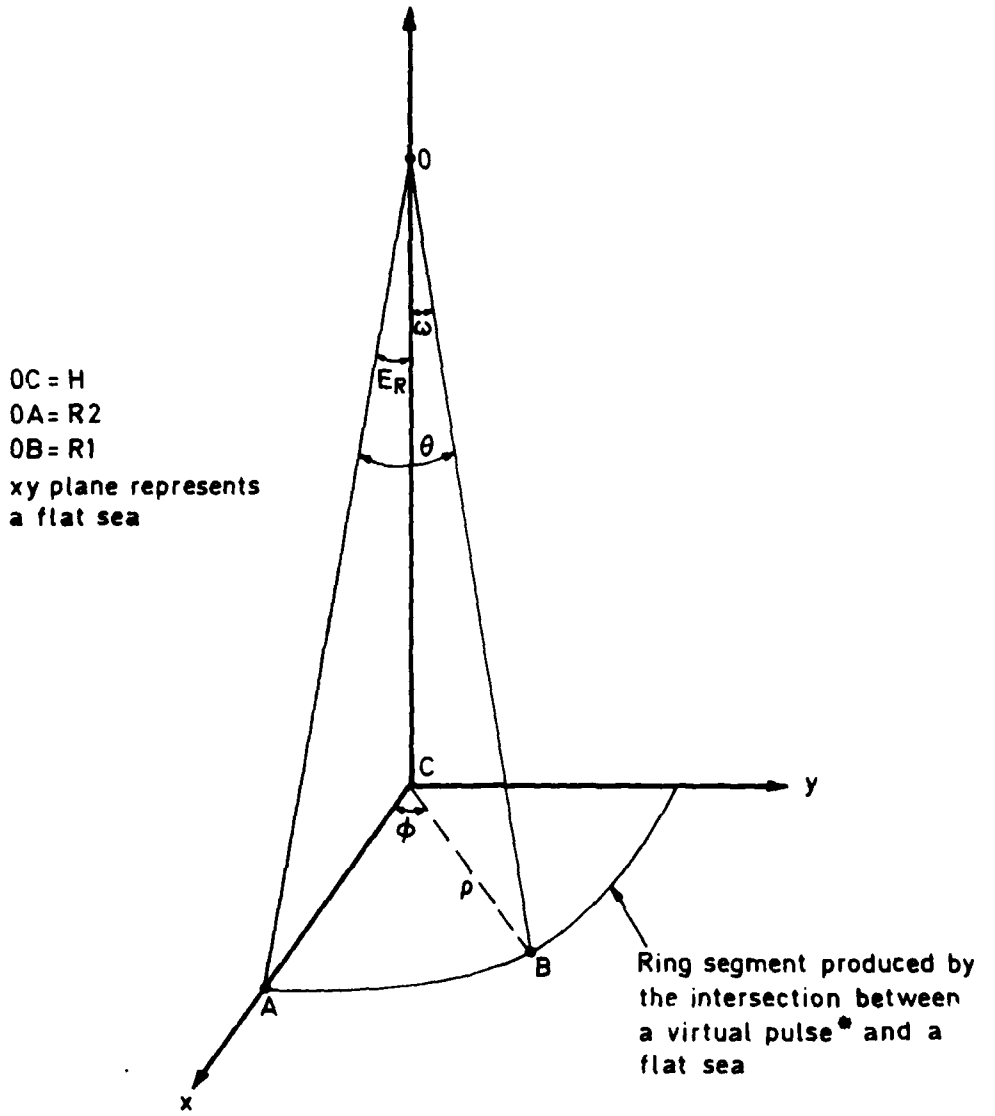

* ie. a pulse of infinitesimal width

Fig 6 Geometry for a pulse return from a flat sea surface

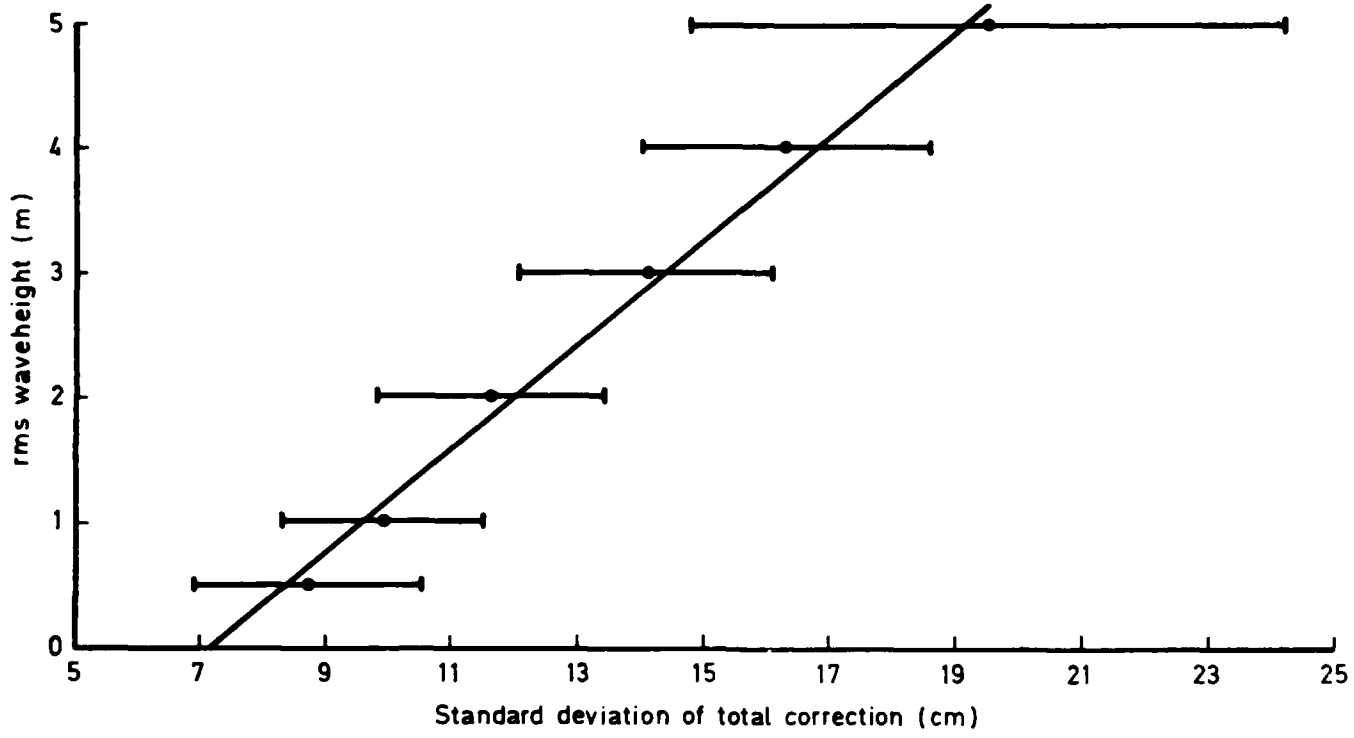

Fig 7 *Accuracy of the true altitude measurements derived from Seasat 1 altimeter data*

Fig 7

[redacted]

[redacted]

As far as possible this page should contain only unclassified information. If it is necessary to enter classified information, the box concerned must be marked to indicate the classification, e.g. (S), (C) or (R).

1. DRIC Reference (to be added by DRIC)	2. Originator's Reference RAE TR 82059	3. Agency Reference N/A	4. [redacted]
5. DRIC Code for Originator 7673000W	6. Originator (Corporate Author) Name and Location Royal Aircraft Establishment, Farnborough, [redacted]		
5a. Sponsoring Agency's Code N/A	6a. Sponsoring Agency (Contract Authority) Name and Location N/A		

7. Title: The accuracy of Skeet 1 altimeter altitude measurements under dynamic and static conditions

7a. (For Translations) Title in Foreign Language

7b. (For Conference Papers) Title, Place and Date of Conference

8. Author 1: Surname, Initials Whitby, G.C.	9a. Author 2 -	9b. Authors 3, 4 [redacted]	10. [redacted]
11. Contract Number N/A	12. Period N/A	13. [redacted]	

14. [redacted]

15. [redacted]

16. [redacted]

17. [redacted]


DA
FILM